

Effect of background winds on vertical wavenumber spectra of atmospheric gravity waves

Stephen D. Eckermann

Computational Physics, Incorporated, Fairfax, Virginia, and E. O. Hulburt Center for Space Research
Naval Research Laboratory, Washington, D. C.

Abstract. Observations of quasi-invariant m^{-3} power spectra of various atmospheric perturbations at large vertical wavenumbers m have received considerable theoretical attention. Yet some other observations, most notably in the stratosphere, have revealed significant departures from this shape and much reduced spectral densities at large m . Here it is argued that these changes arise when a spectrum of gravity waves encounter mean wind changes which cause intrinsic horizontal phase speeds to increase. Concomitant changes in vertical wavenumbers, amplitudes, and shear variance can produce changes in spectral character qualitatively similar to observations. The two important dynamical processes governing the spectral response are refraction of vertical wavenumbers and conservation of Eliassen-Palm flux for nondissipating waves, processes already encapsulated in both single-wave and spectral parameterizations of gravity-wave processes. Retrospective application of these ideas to various observations in the literature leads to successful “prediction” (based on the background wind profile) of either quasi-invariant m^{-3} spectra or attenuated spectra at large m . However, while explaining their occurrence, the precise changes in spectral shape predicted by simple models of wind-shifted spectra often differ from those observed.

Introduction

Spectral analysis of vertical profiles of horizontal-velocity (u'), relative-temperature and relative-density fluctuations in the atmosphere reveal wavenumber power spectra of the form $\alpha A(N)m^{-q}$ at large wavenumbers m , where N is the background Brunt-Väisälä frequency N , $A(N)$ is a polarization factor which depends on the atmospheric variable being measured (e.g., $A(N) = N^2$ for u' data), and α is a constant. Early data suggested $q \sim 2.4$ [Van Zandt, 1982], but a range of later measurements suggested near-constant values of $q = 3$ and $\alpha \sim 1/10$ - $1/6$ [e.g., Smith et al., 1987; Fritts et al., 1988; Tsuda et al., 1989; Wu and Widdel, 1989, 1991].

Since then, a number of models have been developed which seek to explain these quasi-invariant spectral shapes. Currently, they can be grouped into three main categories [e.g., Hines, 1993a]: (model a) saturation models, in which the spectral shape is due to saturated wave amplitudes [e.g., Dewan and Good, 1986; Smith et al., 1987]; (model b) Doppler-spread models, in which the shape arises from stochastic wavenumber spreading of large- m waves by the velocity oscillations of smaller- m waves [Hines, 1991b, 1993b]; and (model c) diffusive models, in which nonlinear interactions among the waves act diffusively upon the wave ensemble to yield an m^{-3} spectral shape [e.g., Weinstock, 1990; Gardner, 1994; Zhu, 1994]. These classifications are somewhat arbitrary, as there are similarities and differences among these and other proposed models [e.g., Müller et al., 1986; Dewan, 1994; Sato and Yamada, 1994].

However, recent higher-resolution measurements, performed throughout the year at different locations and alti-

tudes, have on occasion revealed greater variations in the large- m portion of the spectrum than most models currently allow. Most notably, the spectra at large m in the stratosphere are often (although not always) less intense ($\alpha \sim 1/60$ - $1/20$) and shallower or steeper than expected ($q \neq 3$) [e.g., Shibata et al., 1988; Wilson et al., 1990, 1991b; Tsuda et al., 1991, 1994b; Senft et al., 1993; Hostetler and Gardner, 1994; Mitchell et al., 1994; Whiteway and Carswell, 1994; Allen and Vincent, 1995]. These features, when they arise, tend to be persistent and climatological rather than transitory [e.g., Tsuda et al., 1991; Wilson et al., 1991b]. Some mesospheric data also exhibit spectral shape and intensity variations at large m which exceed model constraints, although here the form and occurrence of the spectral changes seem more random and less climatologically reproducible [e.g., Wu and Widdel, 1990; Senft and Gardner, 1991; Collins et al., 1994].

Some theoretical spectral models have already been applied or adapted to account for these observations. Using the saturation hypothesis, some have argued that attenuated shallow spectra such as these indicate an unsaturated wave field [e.g., Tsuda et al., 1991], while others have argued that they may reflect dynamical saturation of inertia gravity waves [e.g., Shibata et al., 1988; Wilson et al., 1990]. Hines [1993a] showed that similar-looking spectral variations can arise within a Doppler-spreading framework by considering input source spectra of different forms. Similar effects are accommodated within the wave-diffusive model of Weinstock [1990].

While illustrating that spectral variations are theoretically possible at large m , these arguments did not identify the physical processes responsible for the presence or absence of an attenuated spectrum in a given region of the atmosphere. The first theory to attempt this was developed by Kuo and Lue [1994], who proposed that the presence of vertical

Copyright 1995 by the American Geophysical Union.

Paper number 95JD00987.
0148-0227/95/95JD-00987\$05.00

Report Documentation Page

Form Approved
OMB No. 0704-0188

Public reporting burden for the collection of information is estimated to average 1 hour per response, including the time for reviewing instructions, searching existing data sources, gathering and maintaining the data needed, and completing and reviewing the collection of information. Send comments regarding this burden estimate or any other aspect of this collection of information, including suggestions for reducing this burden, to Washington Headquarters Services, Directorate for Information Operations and Reports, 1215 Jefferson Davis Highway, Suite 1204, Arlington VA 22202-4302. Respondents should be aware that notwithstanding any other provision of law, no person shall be subject to a penalty for failing to comply with a collection of information if it does not display a currently valid OMB control number.

1. REPORT DATE JUL 1995		2. REPORT TYPE		3. DATES COVERED 00-00-1995 to 00-00-1995	
4. TITLE AND SUBTITLE Effect of background winds on vertical wavenumber spectra of atmospheric gravity waves				5a. CONTRACT NUMBER	
				5b. GRANT NUMBER	
				5c. PROGRAM ELEMENT NUMBER	
6. AUTHOR(S)				5d. PROJECT NUMBER	
				5e. TASK NUMBER	
				5f. WORK UNIT NUMBER	
7. PERFORMING ORGANIZATION NAME(S) AND ADDRESS(ES) Naval Research Laboratory, E.O. Hulburt Center for Space Research, Washington, DC, 20375				8. PERFORMING ORGANIZATION REPORT NUMBER	
9. SPONSORING/MONITORING AGENCY NAME(S) AND ADDRESS(ES)				10. SPONSOR/MONITOR'S ACRONYM(S)	
				11. SPONSOR/MONITOR'S REPORT NUMBER(S)	
12. DISTRIBUTION/AVAILABILITY STATEMENT Approved for public release; distribution unlimited					
13. SUPPLEMENTARY NOTES					
14. ABSTRACT see report					
15. SUBJECT TERMS					
16. SECURITY CLASSIFICATION OF:			17. LIMITATION OF ABSTRACT	18. NUMBER OF PAGES	19a. NAME OF RESPONSIBLE PERSON
a. REPORT unclassified	b. ABSTRACT unclassified	c. THIS PAGE unclassified			

shear in the background wind triggered attenuated spectra. They argued that differential horizontal advection of vertical parcel oscillations due to the wave is induced by the background wind shear and leads to reduced spectral intensities in the horizontal-velocity spectrum. *Zhu* [1994], on the other hand, argued that $q < 3$ arose in the stratosphere when radiative damping exceeded diffusive damping of the wave spectrum.

Here another theory is proposed, in which attenuated spectra arise due to changes in background wind speeds, which refract waves to smaller vertical wavenumbers and produce accompanying reductions in the total shear variance and vertical wave-action flux of the wave field. Here we shall discuss these ideas within the context of spectral models *a* and *b* only, as they are the most obviously different from each other [*Hines*, 1991a]. In the development it will hopefully become clear that this mechanism is sufficiently general and robust in nature that it should produce qualitatively similar spectral responses within the framework of model *c* or any other wave spectral theory.

Indeed, these refraction processes have been encapsulated mathematically within parameterizations of gravity-wave processes for general circulation models [e.g., *Lindzen*, 1981, 1985; *Fritts and Lu*, 1993; *Lu and Fritts*, 1993]. Thus for the most part we shall either apply or adapt these formulae to illustrate anticipated spectral effects. The major effort is to present a persuasive case for a connection between theoretical changes in spectral shape induced by changes in the background wind speed, and the occurrence or otherwise of reduced spectral densities at large m in the observational literature.

Wind-Shifting Theory

Basic Theory for a Single Wave

In common with the approximations used in developing models *a* and *b* [*Smith et al.*, 1987; *Hines*, 1991b], we shall assume hydrostatic gravity waves in a nonrotating atmosphere. Such waves obey the simple dispersion relation $m^2 = \kappa^2 N^2 / \omega^2$, where κ is the horizontal wavenumber and ω is the intrinsic frequency. Given that $\omega = \kappa(c_h - \bar{U} \cos \varphi)$ by definition, where c_h is the ground-based horizontal phase speed, \bar{U} is the background horizontal wind speed, and φ is the angle between $\vec{\kappa}$ and \vec{U} , then

$$m = \frac{N}{|c_h - \bar{U} \cos \varphi|}. \quad (1)$$

The denominator $|c_h - \bar{U} \cos \varphi|$ is the intrinsic horizontal phase speed of the wave, $|c_h^{\text{int}}| = |\omega/\kappa|$.

We shall assume that horizontal and temporal variations in the background atmosphere are negligible, so that κ and c_h remain constant as a given wave propagates upward [e.g., *Eckermann*, 1992]. Since in the absence of dissipation the wave also conserves its Eliassen-Palm (EP) flux $\rho_0 u' w'$, where ρ_0 is the background density and w' is the vertical velocity perturbation [*Eliassen and Palm*, 1960], it follows that the horizontal-velocity variance $\overline{u'^2}$ varies with height z approximately as

$$\overline{u'^2} = \overline{u_0'^2} \frac{m}{m_0} \exp \left(\int_{z_0}^z dz / H_u \right), \quad (2)$$

where m_0 and $\overline{u_0'^2}$ are the wavenumber and horizontal-velocity variance, respectively, at height z_0 , and H_u is the density scale height [e.g., *Lindzen*, 1981; *Schoeberl*, 1985b]. Using (1) and assuming that N is constant, (2) can be reexpressed as [*Lindzen*, 1981]

$$\overline{u'^2} = \overline{u_0'^2} \exp \left(\int_{z_0}^z dz / H_u \right), \quad (3)$$

where

$$\frac{1}{H_u} \approx \frac{1}{H_\rho} + \frac{1}{c_h - \bar{U} \cos \varphi} \frac{d}{dz} \bar{U} = \frac{1}{H_\rho} + \frac{1}{H_\sigma}. \quad (4)$$

The scale height for $\overline{u'^2}$, H_u , quantifies the compensating interchange of variance between $\overline{u'^2}$ and $\overline{w'^2}$ in order to maintain both the dispersion relation (1) and a conserved EP flux. Similarly, the normalized shear variance $\sigma^2 = m^2 \overline{u'^2} / N^2$, which quantifies the stability of a wave (or, indeed, of a spectrum of waves) [e.g., *Desaubies and Smith*, 1982; *Hines*, 1991a], varies with a scale height H_σ given by

$$\frac{1}{H_\sigma} \approx \frac{1}{H_\rho} + \frac{3}{c_h - \bar{U} \cos \varphi} \frac{d}{dz} \bar{U} = \frac{1}{H_\rho} + \frac{3}{H_\sigma}. \quad (5)$$

It is worth stressing at this point that even though a wind-shear term $d\bar{U}/dz$ appears in (4) and (5), it plays no direct physical role in modifying wave characteristics through the momentum equations, as it can do in other situations [e.g., *Schoeberl*, 1985a; *Hines*, 1989]. Rather, it appears purely due to the reformulation of the vertical variations of $\overline{u'^2}$ as an exponential in (3). Note that when (4) is multiplied by dz in (3), we are left with a term of the form $\Delta \bar{U} = \bar{U}(z + dz) - \bar{U}(z)$, indicating that it is the wind speed variations rather than the shear itself that is the fundamental process here. In contrast, the shear itself is fundamental to the theory of spectral attenuation developed by *Kuo and Lue* [1994].

Figure 1a illustrates how φ relates to the phase velocity \vec{c}_h and wind velocity \vec{U} in the horizontal plane. It reduces to a one-dimensional problem along an axis $Q\vec{O}P$ which is aligned parallel to \vec{c}_h , as depicted in Figure 1b. Consequently, we shall consider, without loss of generality, the limiting case of $\varphi = 0^\circ$ or 180° , so that

$$c_h^{\text{int}} = c_h - \bar{U}, \quad (6)$$

where c_h and \bar{U} can now be positive or negative along the $Q\vec{O}P$ axis in Figure 1b. In most cases that we shall consider, \bar{U} is a zonal wind, and so $Q\vec{O}P$ is aligned east-west.

Thus H_σ can be positive or negative, depending on whether $|c_h^{\text{int}}|$ decreases or increases with height. To monitor this, we introduce the sign parameter

$$\hat{\beta} = \text{sgn} \left(\frac{d}{dz} \frac{\bar{U}}{c_h^{\text{int}}} \right) = \text{sgn} \left(\frac{1}{H_\sigma} \right), \quad (7)$$

with $\hat{\beta}$ defined such that it matches the sign convention of the wind shift parameter β introduced later when analyzing wave spectra.

If $\hat{\beta} = -1$, then $H_\sigma < 0$. This leads, via (3) and (4), to growth of $\overline{u'^2}$ with height which is more gradual than $\exp(\int dz/H_\rho)$, in order to conserve EP flux as the mean

wind varies. For $\hat{\beta} = -1$, the winds also dilate $|c_h^{int}|$ and so reduce m according to (1). This wavenumber decrease is a refraction effect induced by background wind shifts which increase ω . Since we are concerned primarily with wavenumbers here, we shall refer to $\hat{\beta} = -1$ as “downshifting.” These effects are illustrated in Figure 2a for the $c_h = 25 \text{ m s}^{-1}$ wave on the left, propagating in a mean wind environment typical of the winter lower stratosphere at $\sim 55^\circ\text{S}$.

Conversely, the other wave in Figure 2a experiences “upshifting” of vertical wavenumbers m within these background winds (i.e., $\hat{\beta} = +1$), since \bar{U} moves closer to this wave’s c_h value as it propagates upward, so that $|c_h^{int}|$ decreases and m increases. This upshifting leads to positive $H_{\bar{U}}$ values and thus variance growth with height greater than $\exp(\int dz/H_\rho)$, as illustrated.

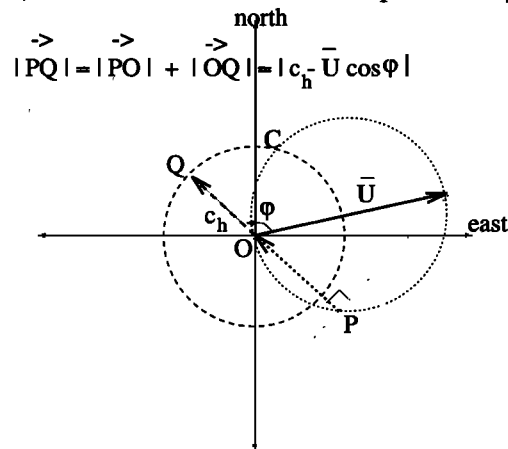
Figure 2b traces the evolution of $\overline{u'^2}$ and m for the $\hat{\beta} = -1$ and $\hat{\beta} = +1$ waves in Figure 2a during their propagation from 10 to 25 km. For the $\hat{\beta} = +1$ wave, both $\overline{u'^2}$ and m increase, whereas both quantities decrease for the $\hat{\beta} = -1$ wave. Effects such as these were first quantified by Lindzen [1985], who investigated their influence on the momentum budget of the lower atmosphere.

Since background wind changes can produce systematic changes in both wave variance and wavenumber, they can influence the shape of the vertical wavenumber power spectrum of horizontal velocities, $F_u(m)$.

Application to the Vertical Wavenumber Spectrum

Fritts and Lu [1993] parameterized the effects of wind shifts on a theoretical wavenumber spectrum based to some extent on a saturation model. However, the dynamical

a) Variation of Intrinsic Phase Speed with ϕ



b) Intrinsic Phase Speed with respect to QOP

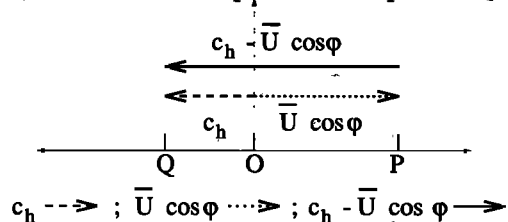


Figure 1. (a) Phasor diagram showing the geometry of $c_h - \bar{U} \cos \phi$ with varying azimuth angle ϕ and (b) the one-dimensional simplification of the problem along QOP .

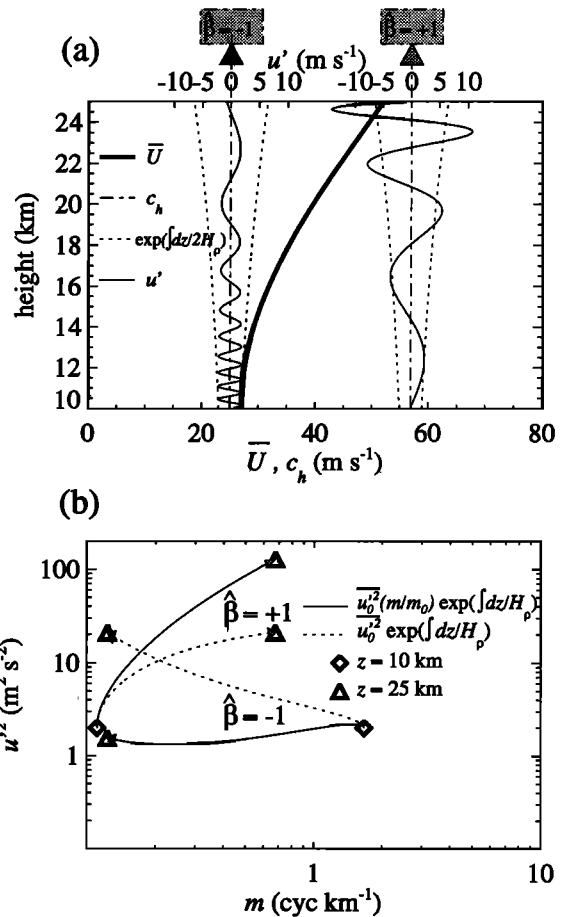


Figure 2. (a) Variation of wave horizontal-velocity oscillations u' (thin solid curve) with height for two waves, centered about their horizontal phase speeds (shown with dashed lines) of $c_h = 25 \text{ m s}^{-1}$ ($\hat{\beta} = -1$) and $c_h = 56.9 \text{ m s}^{-1}$ ($\hat{\beta} = +1$). The wind profile \bar{U} is the thick curve, and the u' variations relative to c_h are shown on the top x axis; $\exp(\int dz/2H_\rho)$ growth of the initial velocity amplitude is plotted with dotted curves, assuming an isothermal background temperature of 215 K; (b) variation of $\overline{u'^2}$ (solid curve) versus m for both waves during propagation from 10 to 25 km. Dotted curves show simple $\exp(\int dz/H_\rho)$ scaling of the initial variance with height.

approach they used to model the effects is similar to the one used by Hines [1991b, 1993b] to describe the evolution of the spectrum under a “Doppler-spreading” model. The Doppler-spreading effect is basically the same as the wind-induced refraction that we have discussed, except that for Doppler spreading, $\Delta \bar{U}$ is due to random velocity fluctuations of larger-scale waves rather than a background wind. This produces statistical spreading of wavenumbers m , as opposed to the systematic shifts induced by a discrete change in the mean wind speed.

The analytical model of the spectrum assumed by Fritts and Lu [1993] in the absence of background wind shifts takes the form

$$F_u^i(m) \propto N^{1/2} e^{z/H_E} \frac{A(m/m_*)}{m_*}, \quad (8)$$

where $A(\mu) = (4/\pi)\mu/(1 + \mu^4)$ and

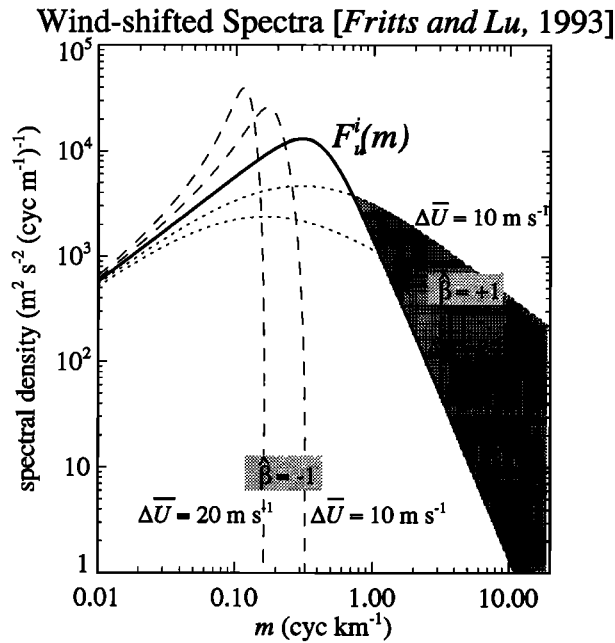


Figure 3. Response of $F_u^i(m)$ (solid curve) to upshifting (dotted curves, $\hat{\beta} = +1$) and downshifting (dashed curves, $\hat{\beta} = -1$), using $\Delta\bar{U}$ values of 10 and 20 m s^{-1} , $N = 0.021 \text{ rad s}^{-1}$ and $m_* = 2\pi/(2.5 \text{ km})$. The shaded region is the excess upshifted spectral density which is scaled back to the spectral saturation limit of $\alpha N^2 m^{-3}$.

$$m_* \propto N^{3/4} e^{-z/H_*}. \quad (9)$$

This is similar to the analytical Doppler-spread spectrum given by Hines [1991b]. Fritts and Lu [1993] assumed that the unshifted spectrum $F_u^i(m)$ was invariant with altitude at $m \gg m_*$, so that $H_E \approx 2H_\rho \approx H_*/2$ and $F_u^i(m) \rightarrow \alpha N^2/m^3$ at $m \gg m_*$, where $\alpha \sim 1/8-1/6$ [Fritts and VanZandt, 1993], in general agreement with the unattenuated observations cited earlier. Under these assumptions, (8) is plotted as the solid curve in Figure 3 using $2\pi/m_* = 2.5 \text{ km}$ and $N \approx 0.021 \text{ rad s}^{-1}$, which are typical values in the lower stratosphere [e.g., Fritts and Chou, 1987; Tsuda et al., 1991; Allen and Vincent, 1995].

To model the effects of wind-induced refraction on the wave spectrum, Fritts and Lu [1993] considered the spectral response to a sudden shift in wind speed $\Delta\bar{U}$, assuming no change in the altitude of observation and ascribing the spectral density $F_u^i(m_i)$ at some m_i to a wave or waves of wavenumber m_i . Their results for $\hat{\beta} = +1$ and $\hat{\beta} = -1$ are shown with dotted and dashed curves, respectively, in Figure 3. The form and degree of spectral variation is controlled by the wind shift parameter

$$\beta = \hat{\beta} \frac{|\Delta\bar{U}|m_*}{N}, \quad (10)$$

which is essentially the same as the β factor arising in models of Doppler-shifted frequency spectra [e.g., Fritts and VanZandt, 1987; Gardner et al., 1993].

As in Figure 2, $\hat{\beta} = -1$ yields reduced wavenumbers (downshifting) and a reduction in the area beneath the spectrum (i.e., reduced variance). The converse is true for $\hat{\beta} = +1$, and Fritts and Lu [1993] argued that the increases in

total variance for $\hat{\beta} = +1$ produced instabilities within the wave field. For example, single-wave velocity perturbations become convectively unstable when $u' > c_h - \bar{U} \cos \varphi$. This occurs at a phase where the $-u'$ perturbations in Figure 2a (which are centered on c_h) cross the \bar{U} curve, as the $\hat{\beta} = +1$ wave does at $z \sim 23.5 \text{ km}$. Saturation models argue that the amplitudes of such waves are attenuated to saturated levels, so that instabilities no longer occur. So, as waves approach a critical level ($|c_h - \bar{U} \cos \varphi| \rightarrow 0$, $m \rightarrow \infty$), they are almost totally dissipated ($u' \rightarrow 0$), although this ignores various nonlinear transmission, reflection, and amplification processes which can arise within these regions [e.g., Maslowe, 1986; Walterscheid and Schubert, 1990].

On the basis of these saturation arguments, Fritts and Lu [1993] concluded that the increases in spectral density at large m for $\hat{\beta} = +1$ (shaded in Figure 3) could not be sustained and so scaled their upshifted spectra back to the $\alpha N^2/m^3$ limit to restore wave field stability. Sato and Yamada [1994] applied saturation processes to a single upshifted wave and derived model upshifted spectra close to this limiting shape.

Doppler-spreading models do not attribute this limiting spectral shape to saturation but rather to the characteristic statistical form that Doppler-spreading effects take in the Fourier domain; but for a spectrum of $\hat{\beta} = +1$ waves, wind shifts lead to increases in both $\overline{u'^2}$ and σ^2 over the whole spectrum, according to (4) and (5). Both of these increases trigger enhanced Doppler spreading of waves to large- m values where they are removed by dissipation [Hines, 1991a, b, 1993b]. Once enough waves have been removed so that σ^2 is reduced to a stable value, Doppler spreading should return the characteristic $\alpha N^2/m^3$ spectrum at large m . Thus as long as these removal processes are sufficiently rapid, then an attenuation of the large- m spectrum for $\hat{\beta} = +1$ waves, which is qualitatively similar to that invoked by Fritts and Lu [1993], should also arise within a Doppler-spreading framework.

Thus to summarize, simple models of refracted wave spectra predict reduced spectral densities ($\alpha < 1/10-1/6$) and steeper spectral indices ($q > 3$) when mean-wind changes yield downshifting ($\hat{\beta} = -1$), whereas conventional $\alpha A(N)m^{-3}$ spectra are anticipated when mean-wind changes are small or yield upshifting ($\hat{\beta} = 0$ or $+1$).

Spectral Observations and the Background Wind Profile

We now review various spectral measurements presented in the literature and reanalyze them with respect to the background wind profile to test whether application of these ideas can account for attenuated and unattenuated spectral data at large m . The survey of the observational literature will be selective rather than exhaustive. The major selection criteria for reanalyzing a given data set are acceptable accuracy (both instrumental and statistical) and knowledge of the background wind profiles accompanying the measurements, to facilitate predictions using the wind-shifting model. Such data will range in character from isolated campaign observations to detailed climatological studies.

Lower Stratosphere

Radiosonde and radar measurements at Kyoto, Japan. A particularly thorough observational study of vertical wave-

number spectra in the lower stratosphere was made possible by high-resolution radar and radiosonde sounding programs conducted at a site near Kyoto (35°N, 136°E) by scientists of the Radio Atmospheric Science Center of Kyoto University. The radar provided velocities, while the radiosondes provided temperature data, and initial intercomparison of the radar measurements of horizontal-velocity spectra and the radiosonde measurements of the spectrum of relative-temperature perturbations T'/T_0 (T' = temperature perturbation, T_0 = background temperature) revealed excellent agreement with theory [Fritts *et al.*, 1988]. Similar analyses were performed on more extensive data sets provided subsequently by these instruments at different times of the year [Tsuda *et al.*, 1989, 1991; Kuo and Lue, 1994].

Tsuda *et al.* [1991] spectrally analyzed over 2 years of the radiosonde data. They found that at large m , the spectra of relative-temperature perturbations and wave-perturbed Brunt-Väisälä frequencies in the stratosphere exhibited similar seasonal variations. Their model for $F_{T'/T_0}^i(m)$ assumed $q = 3$ at large m , with a polarization factor $A(N) = 0.6N^4/g^2$ and $\alpha = 1/6$, which they compared with their measured T'/T_0 spectra. The results are shown in Figure 4, as transcribed from Figure 12 and Table 1 of their paper. While in winter α values were close to (although systematically larger than) model predictions and q was very close to 3, during summer the spectral density at large m was consistently <50% of model predictions, and $q \approx 2.2$ -2.4. Kuo and Lue [1994] analyzed horizontal-velocity spectra using a radar at the same site (the MU radar) and found similar seasonal differences in α . However, while Kuo and Lue [1994] found $q \sim 3$ in winter, their data revealed slightly greater spectral indices ($q \geq 3$) in summer.

Figures 5a and 5b show estimates of the mean zonal winds over this site during winter and summer, respectively. The stratospheric values are balanced wind calculations using climatological temperature and heating rate data from the

Stratospheric Spectra, Kyoto, Japan
[Tsuda *et al.*, 1991]

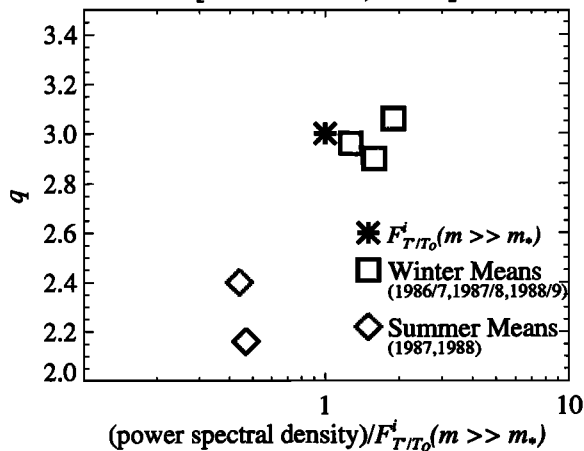


Figure 4. Observed spectral indices q versus observed power spectral densities at large m (normalized by the large- m model spectral density $F_{T'/T_0}^i(m)$) from the radiosonde study of Tsuda *et al.* [1991]. Each point is a seasonal average in a given year, and q was obtained by fitting spectra over the $2\pi/(0.5 \text{ km})$ - $2\pi/(1.4 \text{ km})$ wavenumber interval. The model prediction at large m is asterisked.

Zonal Winds over Kyoto, Japan

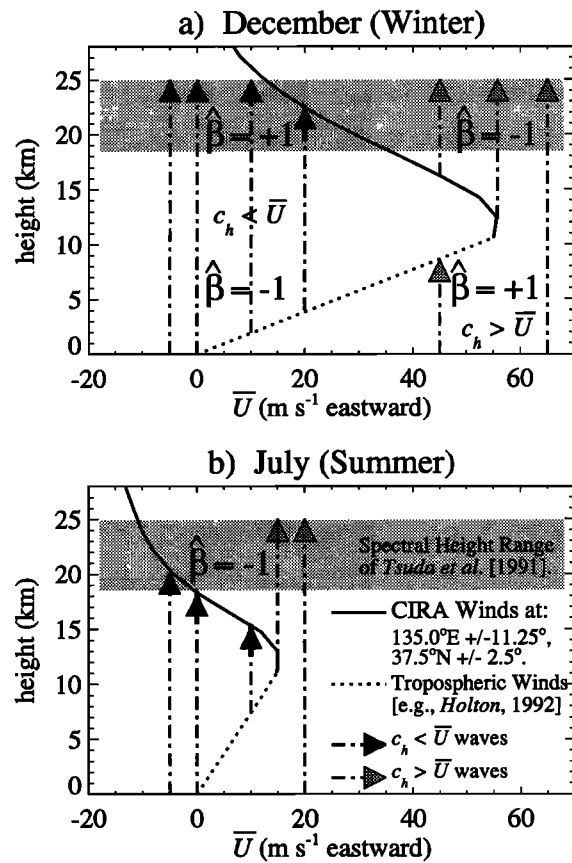


Figure 5. Plots of zonal wind \bar{U} versus height at Kyoto from COSPAR International Reference Atmosphere (CIRA) data (solid curve) and a schematic fit based on climatology (dotted line) (a) during winter and (b) summer. Upward pointing arrows represent upward propagating waves, and their phase speed c_h is given by the x axis velocity to which they point [e.g., Lindzen, 1981]. Waves for which $c_h < \bar{U}$ have dark arrows, whereas $c_h > \bar{U}$ waves have lightly shaded arrows. The shaded strip marks the height interval spectrally analyzed by Tsuda *et al.* [1991].

COSPAR International Reference Atmosphere (CIRA) [Marks, 1989], while the tropospheric profile is a schematic continuation of these data below the 10-km CIRA lower boundary and is based crudely on climatology [Holton, 1992, Figure 6.1]. Temperature profiles were constructed in the same way and were used to convert the wind profiles from log pressure to geometric heights. The height interval over which Tsuda *et al.* [1991] spectrally analyzed their data is shaded.

Waves are depicted on these diagrams with upward pointing vectors at their ground-based horizontal phase speed c_h , as in Figure 2a. As stated earlier, we assume that c_h remains constant with height, and we choose its value on the premise that waves are produced in the troposphere, so that c_h should be of the order of \bar{U} values in tropospheric source regions. A selection of waves for which $c_h < \bar{U}$ (e.g., mountain waves, $c_h \approx 0$) are depicted in Figure 5a with darkly arrowed vectors. The wintertime wind structure allows most of these waves to propagate through the observational height range, as is well known [e.g., Lindzen, 1985;

Schoeberl, 1985a]. The background wind structure produces downshifting ($\hat{\beta} = -1$) of these waves in the troposphere, since $d\bar{U}/dz > 0$ and so \bar{U} moves away from c_h with increasing altitude, whereupon c_h^{int} increases and m decreases. Conversely, in the stratosphere, $d\bar{U}/dz < 0$, leading to upshifting ($\hat{\beta} = +1$) since \bar{U} moves nearer to c_h as the wave propagates upward and m increases, as in Figure 2a. Indeed, *Sato and Yamada* [1994] presented direct evidence of upshifted vertical wavenumbers in radiosonde and MU radar data from these heights during October, when the background-wind profile is similar to Figure 5a.

Waves for which $c_h > \bar{U}$ are shown with lightly shaded arrows in Figure 5a. Lower-tropospheric waves for which $10 \text{ m s}^{-1} \lesssim c_h \lesssim 50 \text{ m s}^{-1}$ cannot enter the stratosphere since they encounter critical levels. However, observations suggest that gravity waves are also produced near the jet stream peak at $\sim 10 \text{ km}$ [e.g., *Hooke and Hardy*, 1975; *Uccellini and Koch*, 1987; *Yamanaka et al.*, 1989; *Fritts and Nastrom*, 1992; *Sato*, 1994], and these waves can enter the stratosphere where they experience downshifting ($\hat{\beta} = -1$).

Observations and modeling indicate that over undular land masses, topographic forcing of gravity waves is more intense than production by other sources [e.g., *Rind et al.*, 1988; *Nastrom and Fritts*, 1992; *Fritts and Nastrom*, 1992; *Bacmeister*, 1993]. On analyzing 4 years of MU radar measurements at heights $\sim 16 \text{ km}$, *Murayama et al.* [1994] found $\overline{u'w'} < 0$ in winter, consistent with $c_h < \bar{U}$ waves. Similar wintertime directions were inferred by *Kitamura and Hirota* [1989] from stratospheric radiosonde profiles over Japan. *Sato* [1994] presented strong evidence that the bulk of the velocity variance observed by the MU radar at $\sim 18\text{--}22 \text{ km}$ during winter was due to mountain waves with c_h values near zero. This indicates that mountain waves (dark arrows) are more energetic than waves emanating from the jet stream (lightly shaded arrows) during winter at this site. However, even if they had similar EP fluxes, Figure 5a reveals that the mountain waves undergo upshifting ($\hat{\beta} = +1$) in the stratosphere while waves from near the jet stream are downshifted ($\hat{\beta} = -1$). This differential refraction yields amplification of the mountain-wave velocity variance relative to the variance of jet-stream-associated waves, as depicted in Figure 2a.

Thus the stratospheric wave variance during winter should be dominated by waves for which $c_h \sim 0$. Since the decrease of the zonal wind with height produces upshifting effects ($\hat{\beta} = +1$) on such a wave field, this will give rise to wave dissipation and a forcing of the spectrum to the $\alpha A(N)m^{-3}$ limit at large m , according to the wind-shifting model. The data of *Tsuda et al.* [1991] support these predictions (see Figure 4).

Figure 5b repeats this analysis for the summertime wind profile. In this case, the $c_h < \bar{U}$ waves, such as mountain waves, cannot propagate into the height range analyzed by *Tsuda et al.* [1991], due to critical-level encounters lower down. *Murayama et al.* [1994] found $\overline{u'w'} \approx 0$ in summertime MU radar observations at $\sim 16 \text{ km}$, a height at which mountain waves can still exist in the data (see Figure 5b). Since $\overline{u'w'} < 0$ for mountain waves, the near-zero $\overline{u'w'}$ values measured by *Murayama et al.* [1994] suggest that $c_h > \bar{U}$ waves also exist at $\sim 16 \text{ km}$ with approximately equal and opposite EP fluxes. On propagating beyond $z \approx 16 \text{ km}$, Figure 5b shows that many waves for which $\overline{u'w'} < 0$ reach critical levels, leaving mainly $c_h > \bar{U}$ ($\overline{u'w'} > 0$) waves at the heights analyzed by *Tsuda et al.* [1991].

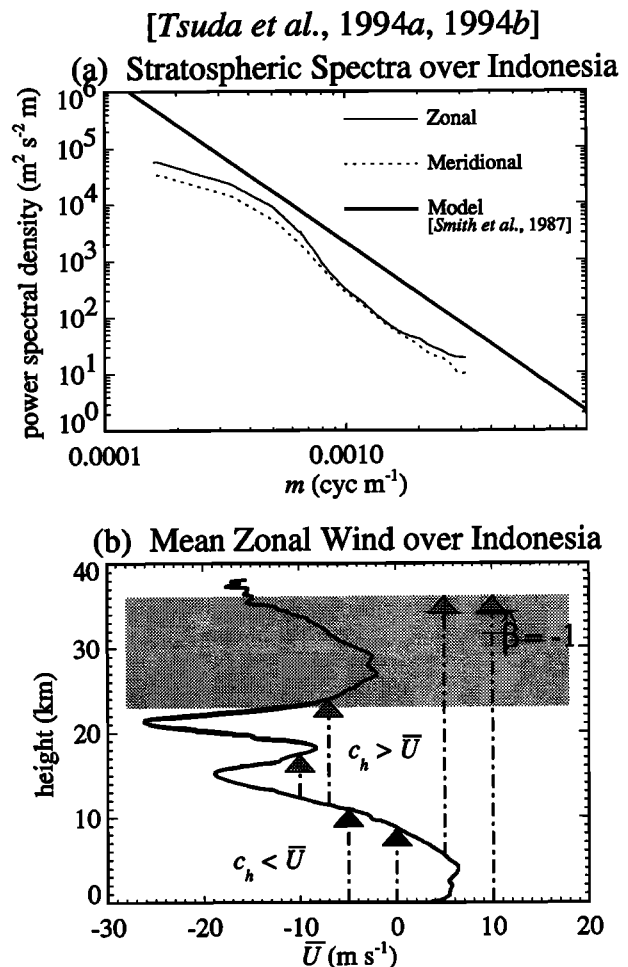


Figure 6. (a) Mean zonal and meridional velocity spectra from 23 to 36 km over Watukosek, Indonesia (7.6°S , 112.7°E), from February 27 to March 22, 1990. The model spectrum of *Smith et al.* [1987] at large m is also plotted. (b) Mean zonal wind as a function of height from the radiosonde data during this period. As in Figure 5, the arrows represent waves, while the shaded region marks the 23- to 36-km band spanned by the data in Figure 6a. The data were transcribed from *Tsuda et al.* [1994a, b].

Thus in summer the stratospheric wave field should be dominated by the eastward phase-speed waves from the jet stream, for which $\hat{\beta} = -1$ since \bar{U} moves away from these c_h values as they propagate through the shaded height range. In these circumstances the wind-shifting model predicts reduced spectral densities at large m , as observed by *Tsuda et al.* [1991] and *Kuo and Lue* [1994]. However, the *Fritts and Lu* [1993] model predicts spectral indices $q > 3$, which agree with the radar results of *Kuo and Lue* [1994] but not the radiosonde findings of *Tsuda et al.* [1991].

Equatorial measurements over Indonesia. *Tsuda et al.* [1994a, b] analyzed radiosonde measurements of horizontal velocities and temperatures from a month-long observational campaign at Watukosek, Indonesia (7.6°S , 112.7°E). *Tsuda et al.* [1994b] noted that stratospheric horizontal-velocity spectra at large m were only 10–25% of model predictions and that $q > 3$. These spectra are reproduced in Figure 6a.

Figure 6b plots the mean background zonal winds, derived from all the measurements during the campaign [*Tsuda et al.*

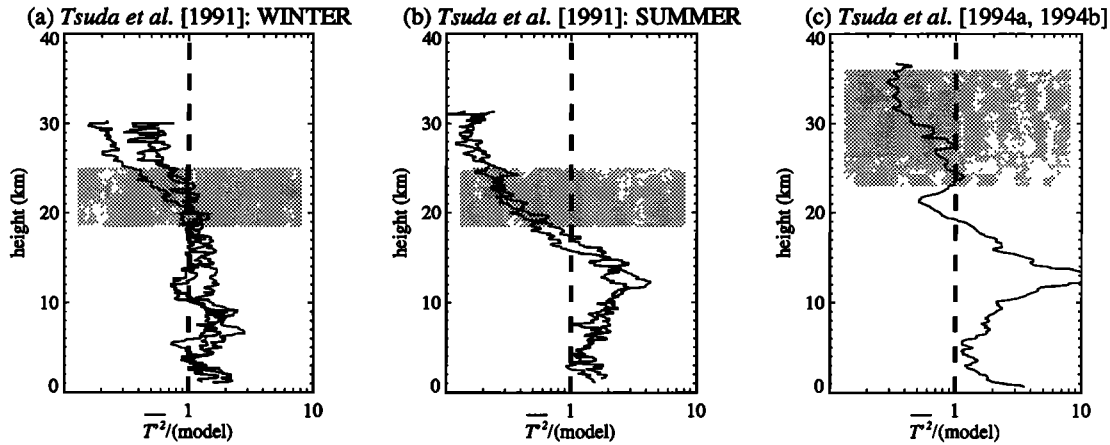


Figure 7. Plots of $\overline{T'^2}$ in the 150- to 900-m range of vertical scales, normalized by model-predicted variances. (a) and (b) Seasonal-mean profiles during winter and summer, respectively, from the observational study of Tsuda *et al.* [1991]. (c) Mean results from the campaign study of Tsuda *et al.* [1994b]. The shaded strips show the height intervals over which data were spectrally analyzed, yielding the results in Figures 4 and 6a. The dashed curve shows model predictions.

al., 1994a, Figure 2]. Following the presentation in Figure 5, the height interval spectrally analyzed by Tsuda *et al.* [1994b] is shaded, and waves for which c_h exceeds (is less than) \bar{U} are plotted with dark (light shaded) vector arrows. The wind-shifting environment is qualitatively similar to that in Figure 5b, where stationary and westward c_h waves reach critical levels, so that mainly eastward phase speed waves reach the stratosphere.

In the 23- to 36-km height range, \bar{U} increases from ~ 23 to 27 km, then decreases from ~ 27 to 36 km. For eastward c_h waves this yields $\hat{\beta} = +1$ at lower heights and $\hat{\beta} = -1$ at the upper heights, and so $\hat{\beta} = -1$ dominates over most of the 23- to 36-km interval. Therefore we anticipate a net downshifting of the spectrum (i.e., $\hat{\beta} = -1$), for which the wind-shifting model predicts reduced spectral densities and $q > 3$ at large m , as observed in Figure 6a. However, strong planetary wave activity in these data [Tsuda *et al.*, 1994a] may also produce time-varying modulation of the wave transmission and wind shifting and hence time-varying modifications of the spectral shape [e.g., Lu and Fritts, 1993].

Allen and Vincent [1995] argued that temperature spectra measured by radiosondes in the stratosphere can be distorted by slow sensor response times, whereas variances tended to be less affected. So, as a further check of these radiosonde data, Figure 7 shows height profiles of the temperature variances at vertical scales between 150 and 900 m. These variances were normalized by the model variance, obtained by integrating $F_T^i(m)$ over the same wavenumber interval [Tsuda *et al.*, 1991, 1994b]. The dashed line shows model predictions. We note that the height variations in the shaded regions of Figures 7b and 7c compare very well with the refractive attenuation of variance predicted using the wind profiles in Figures 5b and 6, respectively. Variances in Figure 7b attenuate above ~ 18 km, a level at which mountain waves are removed by critical levels, leaving mainly downshifted jet stream waves above this level (see Figure 5b). Variances in Figure 7c only fall below model predictions above ~ 28 km, the same height above which downshifting was predicted in Figure 6. The winter profiles in Figure 7a are near model values throughout most of the shaded region,

again consistent with earlier predictions (see Figure 5a). However, values attenuate somewhat at the uppermost heights. This could indicate removal of $c_h < \bar{U}$ waves at these heights, yielding downshifting of $c_h > \bar{U}$ waves, since zonal wind profiles measured by Kitamura and Hirota [1989] and Murayama *et al.* [1994] over Japan often reveal \bar{U} near zero at heights ~ 23 –25 km.

Radiosonde measurements in the southern hemisphere. Allen and Vincent [1995] undertook a detailed statistical study of lower-stratospheric spectra using high-resolution radiosonde temperature measurements from around Australia and Antarctica. Unlike the results of Tsuda *et al.* [1991] from a near-conjugate location in the northern hemisphere, Allen and Vincent [1995] noted little seasonal variability in their spectra. The only location where spectral densities at large m departed significantly from the $\alpha A(N)m^{-3}$ limit was at Davis, Antarctica (69°S , 78°E), where reduced spectral densities and $q < 3$ were observed. All of their spectra were corrected for sensor-response distortion.

Figure 8 shows CIRA zonal wind profiles during summer and winter over two of their radiosonde sites: Davis, Antarctica (69°S , 78°E) and Woomera (31°S , 136°E), a station which lies roughly in the middle of the various Australian radiosonde-launching sites. The height interval spectrally analyzed by Allen and Vincent [1995] is shaded. Figures 8b and 8d reveal that in the winter stratosphere, $d\bar{U}/dz$ differs in sign between Davis and Woomera. Thus during winter, downshifting ($\hat{\beta} = -1$) dominates at Davis, while upshifting dominates at Woomera if $c_h = 0$ waves exist (due to the amplification of upshifted variance relative to the downshifted variance). This is consistent with the attenuated spectra observed at Davis and unattenuated spectra observed at the Australian stations by Allen and Vincent [1995]. Spectral indices q were less than 3 at Davis, whereas the wind-shifting model predicts $q > 3$.

Except for Davis, all data analyzed by Allen and Vincent [1995] came from sites equatorward of 45°S , and all the spectra from these sites tended to $\alpha A(N)m^{-3}$ at large m , in contrast to the attenuated Davis spectra. Figure 9 shows a latitude-height cross section of \bar{U} at 135°E using CIRA July

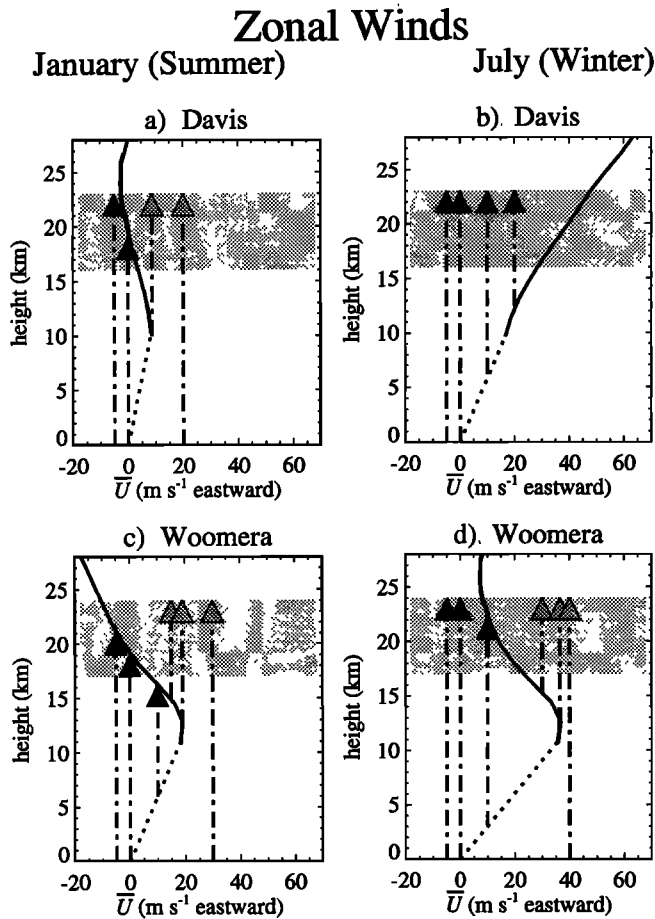


Figure 8. Climatological CIRA zonal winds during (a) and (c) summer and (b) and (d) winter over Davis, Antarctica, and Woomera, Australia. As before, arrows represent waves, while shading marks the regions spectrally analyzed by Allen and Vincent [1995].

(winter) data. The diagram shows that $\bar{U} \geq 0$ throughout most of the lower stratosphere and that $d\bar{U}/dz < 0$ equatorward of 45°S, whereas $d\bar{U}/dz > 0$ poleward of 45°S. According to the wind-shifting model, this will yield downshifted (attenuated) spectra poleward of 45°S (Davis) and upshifted (unattenuated) spectra equatorward of 45°S during winter, as observed by Allen and Vincent [1995]. This assumes that the winter c_h distributions do not vary too much with latitude.

Figures 8a and 8c show the wind profiles during summer, and in these cases wind-shifting predictions are less straightforward. At Woomera, $c_h = 0$ waves enter the shaded height interval but probably cannot propagate much beyond 20 km. Hence a downshifted spectrum dominated by the lightly shaded arrows might be expected, at least above ~20 km, whereas Allen and Vincent [1995] found a seasonally invariant shape near $\alpha A(N)m^{-3}$ at Woomera. The summertime winds at Davis are quite weak, and so one might anticipate a spectrum close to $F_u^i(m)$, yet Allen and Vincent found attenuated spectra which were similar in shape to the winter spectra.

Analysis of these summertime spectra using the wind-shifting model is made difficult by a lack of knowledge of source climatologies (and hence c_h values) in the southern

hemisphere. Topographic forcing is thought to be less intense in the southern hemisphere, although mountainous regions in Australia and Antarctica do produce some stratospheric wave activity [e.g., Bacmeister et al., 1990; Bacmeister, 1993]. Thus wave production by meteorological phenomena in the southern hemisphere [e.g., King et al., 1987; Eckermann and Vincent, 1993; Pfister et al., 1993; Marks and Revell, 1994; Smith et al., 1995] may be more important. Until more is known, our analysis of these summertime spectral findings remains uncertain.

Upper Stratosphere and Lower Mesosphere

Lidar measurements in Wales and France. Climatological data on wave spectra at heights ~30–60 km have been derived from Rayleigh lidar observations at Aberystwyth, Wales (52°N, 4°W), and at two French sites, Biscarosse (44°N, 1°W) and Haute Provence (44°N, 6°E). Case studies of typical spectral shapes were presented by Mitchell et al. [1994] and Wilson et al. [1990, 1991a], and a climatological picture of the space-time variability of spectra from several years of observations with the Welsh and French lidars was given by Marsh et al. [1991] and Wilson et al. [1991b], respectively.

Figure 10 plots CIRA zonal winds at 42.5°N, 0°E using CIRA-balanced winds. The three height intervals spectrally analyzed by Wilson et al. [1990, 1991b] are shaded separately. The diagram shows that intensifying stratospheric winds produce $\hat{\beta} = -1$ waves in the upper stratosphere due to critical-level removal of $\hat{\beta} = +1$ waves, as has been verified observationally [e.g., Hamilton, 1991; Eckermann et al., 1995].

According to the wind-shifting model, this should yield strongly downshifted spectra and attenuated spectral densities at large m in both summer and winter. The data in the height range 30–45 km revealed spectral densities at large m an order of magnitude lower than $F_u^i(m)$ in summer and winter [Wilson et al., 1991b], in line with these predictions. At large m , spectral indices q were ~3 in both seasons, although at smaller m , the q values were smaller and exhibited seasonal variations [Marsh et al., 1991; Wilson et al., 1991b].

The reductions in spectral density due to wind shifting must compete against $\exp(\int dz/H_p)$ growth of $\overline{u'w'}$ for all the waves in the spectrum. While observed spectral densities at large m were larger at 45–60 km than at 30–45 km [Wilson et al., 1991b], they were still below the $\alpha A(N)m^{-3}$ limit. This can occur because downshifting is still significant (i.e., $\hat{\beta} = -1$ and $|\beta| \gg 0$) in this height interval, as evident from Figure 10. Eventually, $\exp(\int dz/H_p)$ growth will produce gravity wave instability and dissipation, and the observed reversal of $d\bar{U}/dz$ in the upper height range 60–75 km in Figure 10 is the well-known sign that gravity wave dissipation is occurring at these levels and above [e.g., Lindzen, 1981; Holton, 1983]. Dissipation implies a spectrum $\alpha A(N)m^{-3}$ at large m according to the saturation model [e.g., Smith et al., 1987; Fritts and Lu, 1993], while for the Doppler-spreading model, it implies that wavenumbers are spread to dissipative scales at large m and that the spectrum relaxes to the $\alpha A(N)m^{-3}$ limit [Hines, 1991b].

The reversal in $d\bar{U}/dz$ due to dissipation of certain waves forces upshifting ($\hat{\beta} = +1$) upon the full spectrum of waves and thus according to the wind-shifting model will continually force the spectrum to the $\alpha A(N)m^{-3}$ limit at lower

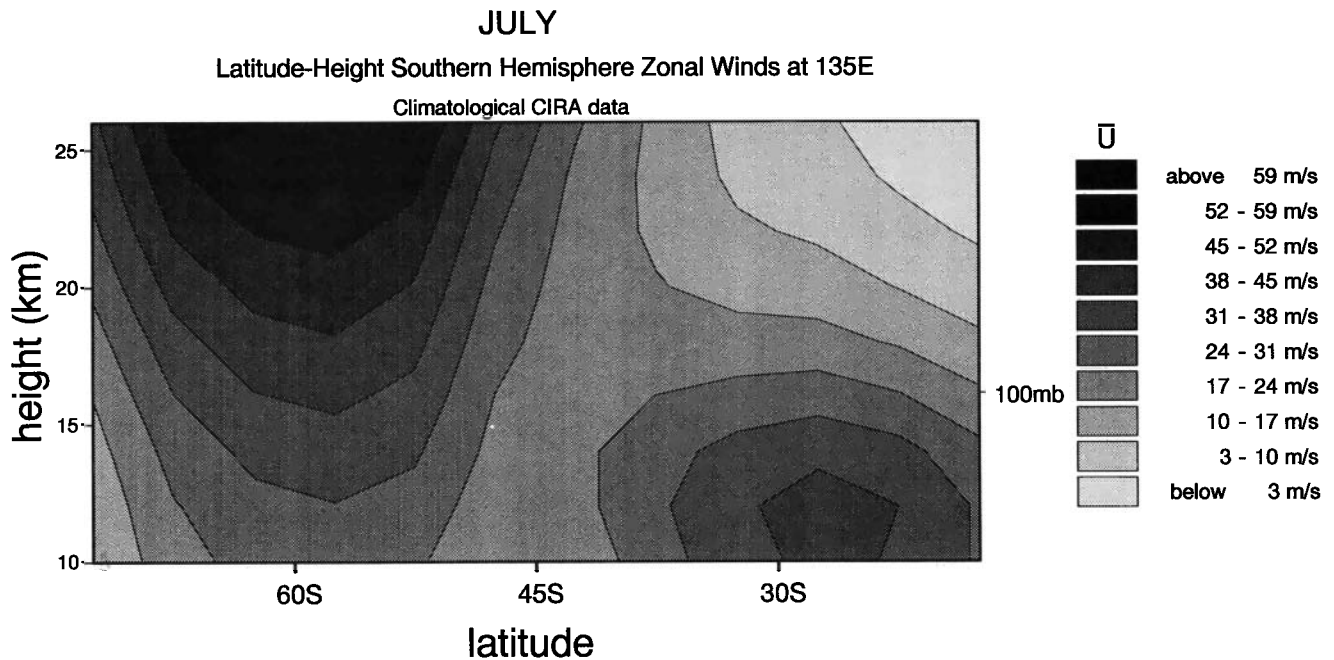


Figure 9. Latitude-height cross section of the CIRA climatological zonal winds in the lower stratosphere at $135^{\circ}\text{E} \pm 12.25^{\circ}$ in the southern hemisphere during July (winter). Darkest shading indicates strong eastward winds and the lightest shading indicates winds near zero (see contour key).

mesospheric heights. *Wilson et al.* [1991b] found that their spectra at 60–75 km attained this limiting form in both winter and summer, in agreement with these wind-shifting predictions.

Case studies from other sites. *Shibata et al.* [1988] analyzed spectra on 12 nights throughout a year at Fukuoka, Japan (34°N , 130°E). Nine of the nights analyzed were from September to December, and they presented mean T'/T_0 spectra within the upper stratosphere (30–49.2 km) and lower mesosphere (45–64.2 km). *Tsuda et al.* [1992] studied horizontal-velocity spectra in the height intervals 22–32 km, 33–43 km, and 47–56 km from rocketsonde experiments over Japan during January–February 1990.

The winds over this site during winter are similar to Figure 10a, except that the tropospheric jet is stronger, winds decrease to near zero at 25–30 km (see Figure 5a), then increase to a peak $\sim 80 \text{ m s}^{-1}$ at 65 km [*Marks*, 1989] before decreasing with height thereafter. However, one should also bear in mind that stratospheric warmings in the winter northern hemisphere can drastically alter this climatological wind structure [e.g., *Labitzke*, 1981]. So, using the winds in Figure 10a as a guide, we anticipate attenuated spectra according to the wind-shifting model, particularly in the 30- to 50-km range. Both *Shibata et al.* [1988] and *Tsuda et al.* [1992] observed attenuated spectral densities in this height range. At large m , *Shibata et al.* [1988] found $q \sim 3$, whereas the data of *Tsuda et al.* [1992] indicated $q > 3$. At the upper height interval, spectra from the lidar (45–64.2 km) and rocketsonde (47–56 km) were closer to the limiting form $\alpha A(N)m^{-3}$, consistent with the reversal of the wind shear at ~ 65 km, and the ensuing onset of upshifting ($\beta = +1$), wave dissipation, and limiting spectral forms at these heights according to the wind-shifting model.

We finish here with some spectral data from Arecibo (18°N , 67°W) that are less easy to interpret. Spectra of

relative-density perturbations ρ'/ρ_0 at 20–45 km, measured by a Rayleigh lidar at Arecibo during January, March, and April 1989, were reported by *Beatty et al.* [1992] and *Senft et al.* [1993]. They found attenuated spectra at large m and spectral indices $q \sim 3$ or slightly less. *Tsuda et al.* [1989] computed horizontal-velocity spectra from Arecibo UHF radar data at ~ 13 –22 km during June 1983 and found spectra close to the $\alpha A(N)m^{-3}$ limit.

The climatological wind profiles for these months are shown in Figure 11. In both cases, waves for which $c_h < \bar{U}$ and $c_h' > \bar{U}$ enter the spectral height interval. There is evidence that mountain waves generated around Arecibo are observed in the radar data [*Hines*, 1989; *Cornish and Larsen*, 1989]. Assuming that they are more energetic than jet-stream-associated waves [e.g., *Fritts and Nastrom*, 1992], then downshifting dominates in Figure 11a and upshifting dominates in Figure 11b, yielding spectral predictions consistent with the observations. However, this presumes that the upshifting of any $c_h > \bar{U}$ waves at upper heights in Figure 11a is not energetically significant, otherwise unattenuated spectra might be expected in both cases.

Mesosphere

In the mesosphere, where the wind shear reverses (see Figure 10), *Senft et al.* [1993] found spectra nearer the $\alpha A(N)m^{-3}$ limit, consistent with wind-shifting predictions (i.e., a change from stratospheric downshifting to mesospheric upshifting). *Hostetler and Gardner* [1994] also observed attenuated stratospheric spectra and unattenuated mesospheric spectra from airborne lidar observations near Hawaii. We shall now analyze more extensive databases of mesospheric spectra to provide better assessments of their relationship to wind-shifting predictions.

Most observations of mesospheric spectra to date have revealed shapes in agreement with the $\alpha A(N)m^{-3}$ limit at

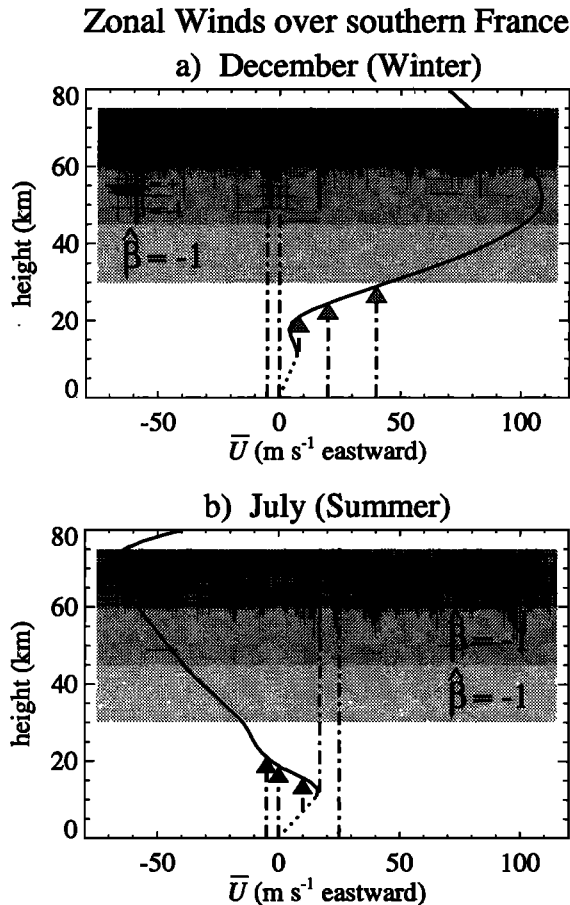


Figure 10. Climatological CIRA zonal winds over southern France ($42.5^{\circ}\text{N} \pm 2.5^{\circ}$, $0^{\circ}\text{E} \pm 12.25^{\circ}$), using the same phenomenological representation as Figure 5. The three shaded strips correspond to the three regions spectrally analyzed by *Wilson et al.* [1991b].

large m [e.g., *Smith et al.*, 1987; *Tsuda et al.*, 1989; *Wu and Widdel*, 1989, 1991]. Since gravity wave dissipation in the mesosphere forces background wind speeds to decrease, and critical-level filtering removes $c_h > \bar{U}$ waves in the stratosphere, then mesospheric gravity waves always tend to be upshifted ($\hat{\beta} = +1$; see Figure 10). In such cases the wind-shifting model predicts the limiting form $\alpha A(N)m^{-3}$ at large m , in accord with observations.

Yet certain situations may give rise to wind profiles in which upshifting does not always occur in the mesosphere [e.g., *Lu and Fritts*, 1993]. According to the wind-shifting model, observations at times of downshifting can produce attenuated spectra, even at these heights. However, because of its height dependence (equation (9)), m_* is smaller at these heights, so that wind shifts $\Delta\bar{U}$ need to be correspondingly larger to produce a given degree of spectral downshifting β , according to (10). Spectral measurements at times of significantly negative β in the mesosphere would provide a powerful test of the wind-shifting theory.

A climatology of lidar spectra at large m in the mesosphere over Urbana (40°N , 88°W) was presented by *Senft and Gardner* [1991]. They noted greater variability in q and α than allowed for within saturation models. This variability, while large, tended to be quasi random. Simultaneous wind

data were not available for direct wind-shifting predictions. Climatological wind patterns measured over Urbana [*Franke and Thorsen*, 1993] suggest upshifted unattenuated spectra.

According to wind-shifting theory, this transient variability suggests that the major wind-shifting influences occur over intraseasonal timescales (i.e., ≈ 1 – 2 months). *Franke and Thorsen* [1993] noted strong tidal activity at these heights, which *Lu and Fritts* [1993] showed can have strong modulating interactions with the gravity wave spectrum. Using $m_* = 2\pi/(13 \text{ km})$ [*Senft and Gardner*, 1991], $N \approx 0.02 \text{ rad s}^{-1}$ [*Senft et al.*, 1994], and typical tidal variations about a mean wind profile, $\Delta\bar{U}$, of $\pm 20 \text{ m s}^{-1}$ [*Franke and Thorsen*, 1993], one obtains β variations of $\sim \pm 0.5$, which may account for some of the quasi-random spectral variability observed by *Senft and Gardner* [1991]. *Thayaparan et al.* [1995] presented direct evidence of tidally modulated gravity wave variances using mesospheric wind data from a nearby site.

Wu and Widdel [1989, 1991] observed $\alpha A(N)m^{-3}$ spectra at large m on spectrally analyzing high-resolution foil-chaff data from ~ 80 – 95 km at Andøya (69°N , 16°E) during July 15, 1987 (summer). Background winds measured during these observations [*Lübken et al.*, 1990] are shown in Figure 12b. They reveal filtering characteristics and mesospheric wind

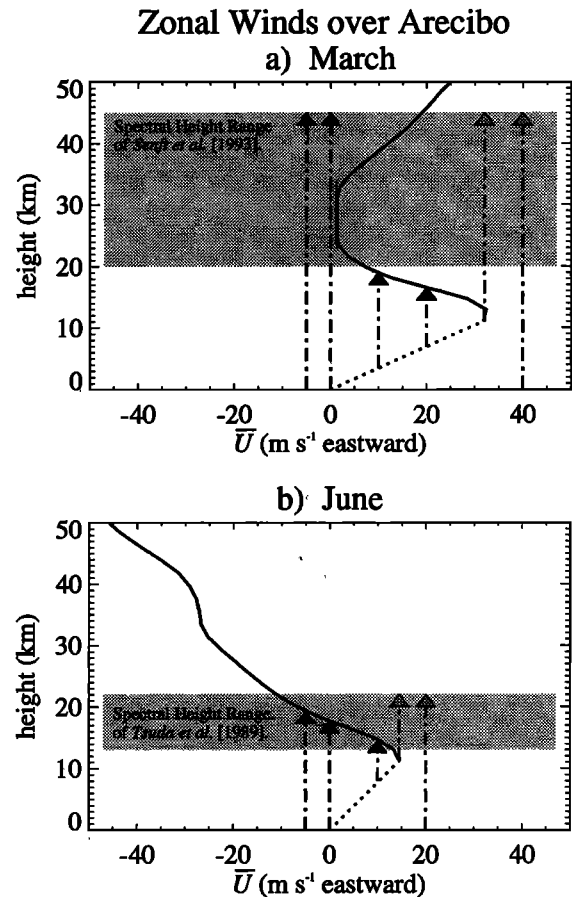


Figure 11. Climatological zonal winds over the region $17.5^{\circ}\text{N} \pm 2.5^{\circ}$, $67.5^{\circ}\text{W} \pm 12.25^{\circ}$ (near Arcibo) for (a) March and (b) June. The height intervals spectrally analyzed by *Senft et al.* [1991] and *Tsuda et al.* [1989] are shaded in Figures 11a and 11b, respectively. Arrows have the same meaning as in Figure 5.

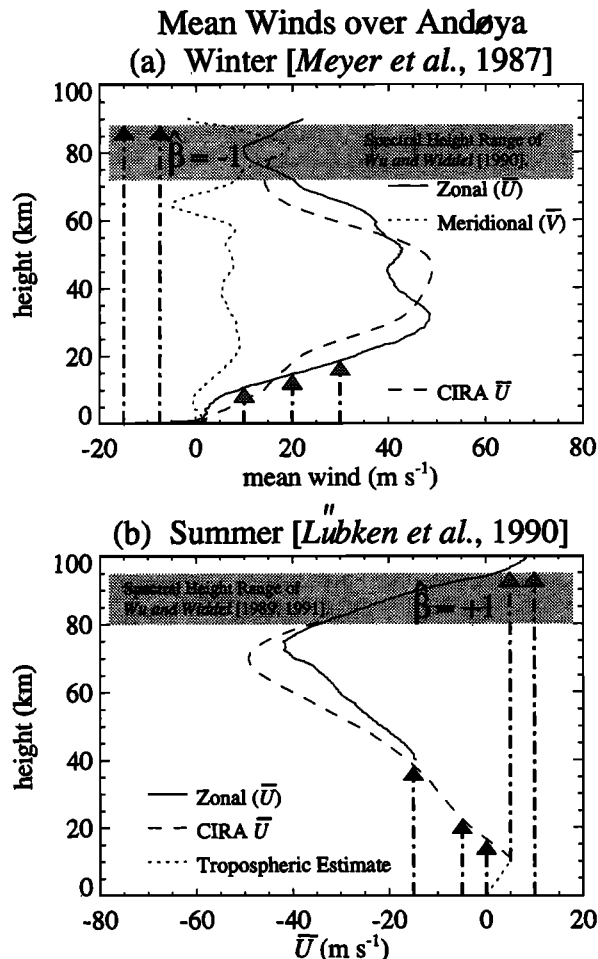


Figure 12. (a) Zonal (solid) and meridional (dotted) winds over Andøya (69°N , 16°E) for January 1984 [Meyer et al., 1987]. The height interval spectrally analyzed by Wu and Widdel [1990] is shaded. (b) Zonal winds at the same location during July 1987 [Lübken et al., 1990]. The height interval spectrally analyzed by Wu and Widdel [1989, 1991] is shaded. CIRA climatological zonal winds are shown with dashed curves in each plot. Arrows have the same meaning as in Figure 5.

patterns which should yield upshifted (unattenuated) spectra, in line with Wu and Widdel's findings.

However, their analysis of data from similar experiments during January-February 1984 (winter) at heights $\sim 72\text{--}88$ km [Wu and Widdel, 1990] revealed a mean $q \sim 2.5$ (as fitted over the vertical-scale range $0.1\text{--}2.1$ km), although spectral shapes and intensities varied considerably among the measurements. The mean January background winds measured during these experiments [Meyer et al., 1987] are shown in Figure 12a along with a climatological CIRA profile [Marks, 1989]. Zonal winds decreased to ~ 79 km, then increased with height thereafter, which should produce downshifting above 79 km. Furthermore, mean meridional winds increased from near zero at 70 km to ~ 20 m s^{-1} at 80 km, which should accentuate a downshifting trend by yielding increasing northward winds acting on a filtered mesospheric wave field containing mainly south-westward c_h values.

The form of the mean wind profiles [Meyer et al., 1987]

raises the possibility that the observation of $q \sim 2.5$ might reflect attenuated (downshifted) mesospheric spectra at these heights and times, in the same way that smaller q values often accompany spectral attenuation in the stratosphere [e.g., Tsuda et al., 1991]. Furthermore, wind speed increases above ~ 79 km themselves may indicate reduced gravity wave dissipation (and hence unsaturated downshifted spectra), since wind speed decreases with height are driven by gravity wave dissipation [e.g., Holton, 1983]. Cause and effect become somewhat blurred in such a picture, but it suggests an intimate association between upshifting (downshifting) and wave dissipation (stability) in the mesosphere.

However, while Wu and Widdel [1990] did not compare their spectra with the limiting $\alpha A(N)m^{-3}$ shape, inspection suggests that their mean spectra do not lie below this model curve. Since there is greater wave activity in these winter data than during summer [e.g., von Zahn and Meyer, 1989], it seems likely that $q < 3$ may often arise here due to the existence of inertial-range turbulence ($q \sim 5/3$) at scales $\leq 300\text{--}600$ m [e.g., Hillert et al., 1994]. Nevertheless, the spectral shapes and intensities measured by Wu and Widdel [1990] varied appreciably from measurement to measurement. Background winds also varied considerably from profile to profile due to stratospheric warmings and tides [Meyer et al., 1987; Röttger and Meyer, 1987], thus yielding time-varying wind shifts which may be responsible for some of this transient spectral variability [e.g., Lu and Fritts, 1993].

The interpretation of these mesospheric data, while admittedly speculative and inconclusive, at least serves to highlight the potential for attenuated mesospheric spectra according to the wind-shifting model.

Troposphere

As in the mesosphere, spectral analyses of tropospheric data generally reveal an unattenuated $\alpha A(N)m^{-3}$ shape at large m [e.g., Tsuda et al., 1991]. Comparison of these observations with wind-shifting predictions is difficult because this is the region where most waves are produced, and so little critical-level filtering of c_h values has yet taken place to enable us to identify whether upshifting or downshifting is preferred. In many situations, both processes probably occur, in which case the upshifted waves will tend to be enhanced in variance relative to the downshifted waves (see Figure 2). A spectrum whose variance is dominated by upshifted waves should produce an $\alpha A(N)m^{-3}$ spectrum at large m , in line with observations. However, the situation will generally be more complicated than this, in which case detailed knowledge of wave phase speeds and the meteorological environment is needed to assess the wind-shifting model properly. Such efforts are beyond the scope of this initial assessment of the process.

Discussion

Comparison With Existing Theories

Saturation models cite attenuated spectra as evidence that the wave field is unsaturated, yet-often there are few clues as to why this should be so. For example, unsaturated spectra in the stratosphere are difficult to reconcile when the spectra observed lower down in the troposphere are saturated [e.g., Tsuda et al., 1991].

The wind-shifting model supports the postulate that the

wave field is unsaturated in such cases and provides a dynamical explanation as to why and where this occurs.

Refractive downshifting ($\beta = -1$) induces spectral attenuation by reducing wavenumbers and, more importantly in this case, attenuating wave-field variances. It produces strong attenuation of the normalized shear variance σ^2 , for which the attenuating effect is approximately triple that for $\overline{u'^2}$ (compare (4) and (5)). It is σ^2 which determines whether the wave field (either one wave or a collection of waves) is saturated [Desaubies and Smith, 1982; Hines, 1991a], and so the reduction of σ^2 by downshifting produces an unsaturated wave field.

This explanation can also be cast within the Doppler-spread theory of Hines [1991b], whereby reductions in $\overline{u'^2}$ over the whole wave spectrum due to downshifting produce reduced spreading of wavenumbers to dissipative vertical scales and reduced σ^2 variances, which imply increased wave field stability.

Hines [1993a] formulated a theory, based on Doppler spreading, to explain attenuated spectral densities in the stratosphere. The idea depends upon the separation of peak vertical wavenumbers in the source spectrum (m_0) and in the Doppler-spread spectrum (m_C , equivalent to m_* in (8)). If $m_C \ll m_0$, then the Doppler-spread spectra tended to the $\alpha A(N)m^{-3}$ shape at $m \gg m_C$ for a variety of source spectra that he considered. However, when $m_C \gg m_0$ for these same source spectra, the resulting Doppler-spread spectra at large m grew with altitude, qualitatively in line with stratospheric observations [e.g., Wilson et al., 1990]. Hines [1993a] coined the latter effect "pseudosaturation." Similar effects can occur within diffusive models of wave spectra [Weinstock, 1990].

Hines [1993a] did not speculate on what processes might produce the necessary conditions (i.e., $m_C \gg m_0$) for pseudosaturated stratospheric spectra [e.g., Wilson et al., 1991b; Senft et al., 1993]. The wind-shifting model can self-consistently trigger or eliminate pseudosaturation conditions in line with observations.

When downshifting occurs, wavenumbers in the source spectrum all decrease, so that the peak wavenumber m_0 of the source spectrum must also decrease. Wind-shifting theory also predicts a reduction in the variance beneath the source spectrum, due to EP-flux conservation. This reduction in $\overline{u'^2}$ leads to reduced Doppler spreading and a consequent increase in m_C [Hines, 1991b]. These oppositely directed wavenumber shifts may then lead to situations where the environment changes from $m_C \ll m_0$ and unattenuated spectra at large m (e.g., in the troposphere), to $m_C \gg m_0$ and attenuated spectra at large m (e.g., due to strong downshifting in the stratosphere), and thereafter to increases in spectral intensity with height until limiting spectral shapes return when $m_C \ll m_0$ is reattained (e.g., in the mesosphere). This may also impact upon the measured spectral index q , as discussed in the next section.

Hostetler and Gardner [1994] measured attenuated stratospheric spectra and also noted an excess of energy at small wavenumbers m . They argued that this may reflect a gravity wave source spectrum dominated by small- m waves produced by geostrophic adjustment of the jet stream, thus accounting for their attenuated spectra via the source-spectrum arguments of Weinstock [1990] and Hines [1993a]. The wind-shifting model can account for these observations without invoking a predominant small- m gravity wave

source. Concentration of energy at small m arises due to refraction of vertical wavenumbers to small values by the background stratospheric winds (e.g., Figure 10), while spectral attenuation follows not only from $m_C \gg m_0$ effects but also from reductions in variance owing to conservation of EP flux under such wind-induced refraction. Indeed, Eckermann et al. [1995] presented direct experimental evidence of refractive downshifting of m values in the upper stratosphere. Furthermore, while the wind-shifting model has been able to account for some observed vertical and seasonal changes in wave spectra through observed changes in the background wind profile, source arguments must invoke a time-varying (and possibly even a height varying) source spectrum to explain these measurements.

Kuo and Lue [1994] proposed a theory which depends upon the term $w' d\bar{U}/dz$ in the linearized zonal momentum equation. This term is often discarded in various approximations, including the ones used here. On integrating general forms of the linearized fluid equations appropriate to gravity waves in a numerical model, Huang et al. [1992] and Kuo et al. [1992] simulated spectra which were similar to observations. To shed light on their findings in regions of wind shear, Kuo et al. [1992] derived an analytical wave shear model based on the $w' d\bar{U}/dz$ interaction effect for a single wave, in which the shear could change $\overline{u'^2}$ with height for a constant $\overline{w'^2}$ value. They found that their model could account for their observed variations of $\overline{u'^2}$ with height. Kuo and Lue [1994] later applied the idea to explain attenuated spectra at large m observed with the MU radar in the lower stratosphere.

In deriving their analytical equations, Kuo et al. [1992] omitted the pressure gradient term in the zonal momentum equation, which is important. When pressure gradient terms are retained in all the momentum equations, one obtains a polarization relation between the peak velocity amplitudes \hat{u}' and \hat{w}' of the form [e.g., Gossard and Hooke, 1975]

$$\hat{u}' = \frac{im - \Gamma + (c_h - \bar{U}) \left(\frac{d}{dz} \bar{U} \right) / C_s^2}{1 - (c_h - \bar{U})^2 / C_s^2} i\hat{w}', \quad (11)$$

where C_s is the speed of sound and $\Gamma = -1/2H_p + g/C_s^2$ is Eckart's coefficient. The dispersion relation, for $d^2/dz^2 \bar{U} = 0$ and ignoring the Earth's rotation, becomes

$$m^2 = \frac{N^2}{(c_h - \bar{U})^2} - k^2 + \frac{2\Gamma}{c_h - \bar{U}} \frac{d}{dz} \bar{U} - \Gamma^2. \quad (12)$$

Note that retaining only the first term in (12) yields (1).

Equations (11) and (12) reveal that the effect of the shear in modifying \hat{u}' in the presence of constant \hat{w}' is only significant when $c_h^{\text{int}} = c_h - \bar{U}$ is large and m is consequently very small. In fact, the effects of the shear are very small for vertical wavelengths $2\pi/m \lesssim 50$ km for typical values of background atmospheric variables and using the largest $d\bar{U}/dz$ values quoted by Kuo et al. [1992]. In light of this analysis, there seems to be no direct way that shearing effects such as these can significantly influence the intensity of the spectrum at the larger vertical wavenumbers, as argued by Kuo and Lue [1994].

Spectral Indices of Attenuated Spectra

A major weakness of the current spectral wind-shifting theory is that while it predicts the occurrence of attenuated

spectra, it has proved less successful in estimating their spectral indices q . The model of *Fritts and Lu* [1993] predicts increases in q to values exceeding 3 (see Figure 3). While this is evident in some spectral data [e.g., *Tsuda et al.*, 1994b], more usually nominal q values ~ 2 – 2.5 are observed [e.g., *Tsuda et al.*, 1991; *Marsh et al.*, 1991; *Senft et al.*, 1993; *Hostetler and Gardner*, 1994; *Mitchell et al.*, 1994].

Fritts and Lu [1993] developed their model with a view to parameterizing gravity wave drag within general circulation models and thus did not formulate it with the analysis of observational spectra in mind. Wind-shifting effects were incorporated in a simple way, whereby the spectral density at each harmonic m_i was associated with a wave or waves of wavenumber m_i , which may not be appropriate. For example, in the Doppler-spreading model, the spectrum at large m is formed by statistical effects and cannot be associated with discrete waves at each m_i [*Allen and Joseph*, 1989; *Hines*, 1991b].

However, while further observations are needed to characterize these q data better, the data to date certainly suggest strongly that in addition to the attenuation of spectral density at large m , downshifting frequently yields a differently shaped spectrum as well (i.e., $q \neq 3$). We shall discuss some possibilities as to how and why shape changes may occur, particularly the occurrence of $q < 3$ which the wind-shifting model employed here does not predict.

As argued earlier, reductions in u'^2 due to downshifting will increase the cutoff wavenumber m_C according to the Doppler-spreading model (or, equivalently, increase m_* according to the saturation model) [*Smith et al.*, 1987; *Hines*, 1991b]. This wavenumber (m_C or m_*) marks a transition zone where the spectral shape changes, from linear variability with m at $m \ll m_C$ or m_* , toward the $\alpha A(N)m^{-3}$ shape at $m \gg m_C$, or m_* [*Hines*, 1991b; see also Figure 3]. Thus an increase in m_C due to the attenuating effects of downshifting acts to move this spectral transition zone to larger wavenumbers. This may explain observations of $q < 3$ at large m for attenuated spectra, since they may now lie within the transition zone where $-1 < q < 3$. This idea differs from the *Fritts and Lu* [1993] model where downshifting also “downshifts” m_* , which is appropriate for instantaneous wind shifts but may not persist once waves grow in amplitude and interact with each other [e.g., *Hines*, 1991b].

Extratropical gravity wave data from the upper stratosphere provide some support for this general scenario. Observations reveal an annual cycle in wave variances, with largest variances in winter and smallest values in summer [*Hirota*, 1984; *Mitchell et al.*, 1991; *Wilson et al.*, 1991b; *Eckermann et al.*, 1995]. As downshifting occurs in both summer and winter (see Figure 10), wind shifting does not cause these seasonal changes in the variance. Instead, they occur mainly through seasonal variations in the $\exp(\int dz/H_p)$ term [*Eckermann*, 1995]. This annual variation of wave variance should produce smaller m_C (m_*) values in winter than in summer, and thus the large- m portion of the spectrum should be closest to the limiting m^{-3} shape in winter, when the inequality $m \gg m_C$ is most likely to be satisfied. Consequently, q should be closest to (farthest from) 3 in winter (summer). Upper stratospheric observations do indeed reveal an annual cycle in q , with q nearest 3 in winter and $q \sim 2$ during summer [*Eckermann*, 1990b; *Marsh et al.*, 1991]. Given that $q \rightarrow 3$ as variances increase into the mesosphere, as discussed earlier, then there appears

to be evidence of a correlation between reduced (increased) variances and q values smaller than (close to) 3, which is somewhat consistent with associated shifts in m_C (m_*).

Thus even though the seasonal variance asymmetry discussed above is not caused by wind shifting, attenuation of variance by wind shifting can produce similar sorts of effects and thus may account for the $q < 3$ data. These arguments assume that a characteristic m^{-3} spectrum (either saturated or pseudosaturated) always returns at $m \gg m_C$, in line with current theories [e.g., *Smith et al.*, 1987; *Allen and Joseph*, 1989; *Hines*, 1991b, 1993a]. Yet some of the observations suggest statistically significant measurements of $q \neq 3$ at m values much larger than predicted m_C values [e.g., *Wu and Widdel*, 1990; *Tsuda et al.*, 1991].

We have only considered waves propagating parallel to the background wind, whereas waves will exist at various angles φ with respect to the background flow (see Figure 1a). More complete theoretical studies of three-dimensional propagation of a wave spectrum within different types of background wind profiles will be needed to anticipate the full effects of these wind-shifting processes on spectral densities and shapes [e.g., *Müller et al.*, 1986; *Huang et al.*, 1992; *Sato and Yamada*, 1994]. The wind-induced changes in variance with height (e.g., Figure 7) imply a highly nonstationary data series, which can also produce important changes in spectral shapes [*Eckermann*, 1990a], as can other data-dependent effects such as time averaging and aliasing [e.g., *Lefrère and Sidi*, 1990; *Gardner et al.*, 1993].

Summary and Conclusions

Here it has been proposed that the occurrence of attenuated vertical-wavenumber spectral densities at large m in the observational literature is caused by the specific nature of the vertical profile of background wind velocity within and beneath the observed region. When attenuated spectra occur, the background winds \bar{U} are such that certain waves are removed from the spectrum through critical-level effects lower in the atmosphere. This leaves a directional wave field higher in the atmosphere for which either $c_h < \bar{U}$ or $c_h > \bar{U}$ is preferred.

Attenuated spectra are observed when the shear is such that \bar{U} “moves away” from c_h as the waves propagate upward, and so vertical wavenumbers $m \approx N/c_h - \bar{U} \cos \varphi$ decrease. This is the “ $\hat{\beta} = -1$ ” (downshifting) scenario, where $\hat{\beta}$ is defined by (7). On the other hand, little spectral attenuation and shape variability is observed in the $\hat{\beta} = +1$ (upshifting) case, where m values increase with height due to \bar{U} moving closer to phase speeds c_h as the waves propagate upward.

Theoretically, changes in \bar{U} which yield $\hat{\beta} = -1$ also produce attenuated wave field variances (to conserve EP flux) and reduced vertical wavenumbers (due to refraction). Application of these ideas to spectral models leads to reductions in spectral densities and changes in spectral shape at large vertical wavenumbers m [*Fritts and Lu*, 1993] which are in qualitative accord with observations. When $\hat{\beta} = +1$, variances and wavenumbers increase, triggering instabilities which lead to dissipation of wave variances back to marginally stable (saturated) values. In such cases, unattenuated spectral shapes at large m are expected and tend to be found in observational data.

Consequently, the wind-shifting theory outlined here,

while admittedly simplistic, nevertheless succeeds in modeling the occurrence and qualitative form of vertical wave-number spectra at large m observed within different background environments. These findings, if taken as valid, can be viewed as initial observational support for efforts to incorporate wind-shifting effects into spectral parameterizations of gravity wave variability within the middle atmosphere [Fritts and Lu, 1993]. Indeed, these wind-shifting processes are spectral analogs of the refraction and dissipation effects for single waves considered by Lindzen [1985]. However, the precise changes in spectral shape at large m are not always well predicted by the current models of wind-shifted spectra (e.g., the spectral index q). Therefore further observational and theoretical studies are needed to fully gauge the extent to which wind-shifting ideas can explain observed spectral variability at large m .

Acknowledgments. I thank Simon Allen for helpful correspondence about his radiosonde investigations and Bryan Lawrence, Rupert Allison and Kip Marks for access to their MADPO software which generated the CIRA-balanced winds used in this paper and which also produced Figure 9. This study owes most to continuing dedicated efforts of ground-based measurement teams around the world, whose ever-improving measurements of wave spectra provided the impetus for this paper. Thanks also to Julio Bacmeister and Mike Summers for their feedback on the manuscript and to Mary Anderson at Computational Physics for her administrative support. This research was partially supported by the Naval Research Laboratory's Atmosphere Remote Sensing and Assessment Program (ARSAP), which is funded by the joint Department of Defence and Department of Energy Strategic Environmental Research and Development Program (SERDP).

References

- Allen, K. R., and R. I. Joseph, A canonical statistical theory of oceanic internal waves, *J. Fluid Mech.*, 204, 185–228, 1989.
- Allen, S. J., and R. A. Vincent, Gravity-wave activity in the lower atmosphere: Seasonal and latitudinal variations, *J. Geophys. Res.*, 100, 1327–1350, 1995.
- Bacmeister, J. T., Mountain-wave drag in the stratosphere and mesosphere inferred from observed winds and a simple mountain-wave parameterization scheme, *J. Atmos. Sci.*, 50, 377–399, 1993.
- Bacmeister, J. T., M. R. Schoeberl, L. R. Lait, P. A. Newman, and B. Gary, ER-2 mountain wave encounter over Antarctica: Evidence for blocking, *Geophys. Res. Lett.*, 17, 81–84, 1990.
- Beatty, T. J., C. A. Hostetler, and C. S. Gardner, Lidar observations of gravity waves and their spectra near the mesopause and stratopause at Arecibo, *J. Atmos. Sci.*, 49, 477–496, 1992.
- Collins, R. L., A. Nomura, and C. S. Gardner, Gravity waves in the upper mesosphere over Antarctica: Lidar observations at the South Pole and Syowa, *J. Geophys. Res.*, 99, 5475–5485, 1994.
- Cornish, C. R., and M. F. Larsen, Observations of low-frequency inertia-gravity waves in the lower stratosphere over Arecibo, *J. Atmos. Sci.*, 46, 2428–2439, 1989.
- Desaubies, Y., and W. K. Smith, Statistics of Richardson number and instability in oceanic internal waves, *J. Phys. Oceanogr.*, 12, 1245–1259, 1982.
- Dewan, E. M., The saturated-cascade model for atmospheric gravity wave spectra, and the wavelength-period (W-P) relations, *Geophys. Res. Lett.*, 21, 817–820, 1994.
- Dewan, E. M., and R. E. Good, Saturation and the “universal” spectrum for vertical profiles of horizontal scalar winds in the atmosphere, *J. Geophys. Res.*, 91, 2742–2748, 1986.
- Eckermann, S. D., Effects of nonstationarity on spectral analysis of mesoscale motions in the atmosphere, *J. Geophys. Res.*, 95, 16,685–16,703, 1990a.
- Eckermann, S. D., *Atmospheric Gravity Waves: Observations and Theory*, Ph.D. thesis, University of Adelaide, Adelaide, Australia, 1990b.
- Eckermann, S. D., Ray-tracing simulation of the global propagation of inertia gravity waves through the zonally averaged middle atmosphere, *J. Geophys. Res.*, 97, 15,849–15,866, 1992.
- Eckermann, S. D., On the observed morphology of gravity-wave and equatorial-wave variance in the stratosphere, *J. Atmos. Terr. Phys.*, 57, 105–134, 1995.
- Eckermann, S. D., and R. A. Vincent, VHF radar observations of gravity-wave production by cold fronts over southern Australia, *J. Atmos. Sci.*, 50, 785–806, 1993.
- Eckermann, S. D., I. Hirota, and W. K. Hocking, Gravity wave and equatorial wave morphology of the stratosphere derived from long-term rocket soundings, *Q. J. R. Meteorol. Soc.*, 121, 149–186, 1995.
- Eliassen, A., and E. Palm, On the transfer of energy in stationary mountain waves, *Geophys. Publ.*, 22(3), 1–23, 1960.
- Franke, S. J., and D. Thorsen, Mean winds and tides in the upper middle atmosphere at Urbana (40°N, 88°W) during 1991–1992, *J. Geophys. Res.*, 98, 18,607–18,615, 1993.
- Fritts, D. C., and H.-G. Chou, An investigation of the vertical wavenumber and frequency spectra of gravity wave motions in the lower stratosphere, *J. Atmos. Sci.*, 44, 3610–3624, 1987.
- Fritts, D. C., and W. Lu, Spectral estimates of gravity wave energy and momentum fluxes, II, Parameterization of wave forcing and variability, *J. Atmos. Sci.*, 50, 3695–3713, 1993.
- Fritts, D. C., and G. D. Nastrom, Sources of mesoscale variability of gravity waves, II, Frontal, convective, and jet stream excitation, *J. Atmos. Sci.*, 49, 111–127, 1992.
- Fritts, D. C., and T. E. VanZandt, Effects of Doppler shifting on the frequency spectra of atmospheric gravity waves, *J. Geophys. Res.*, 92, 9723–9732, 1987.
- Fritts, D. C., and T. E. VanZandt, Spectral estimates of gravity wave energy and momentum fluxes, I, Energy dissipation, acceleration, and constraints, *J. Atmos. Sci.*, 50, 3685–3694, 1993.
- Fritts, D. C., T. Tsuda, T. Sato, S. Fukao, and S. Kato, Observational evidence of a saturated gravity wave spectrum in the troposphere and lower stratosphere, *J. Atmos. Sci.*, 45, 1741–1759, 1988.
- Gardner, C. S., Diffusive filtering theory of gravity wave spectra in the atmosphere, *J. Geophys. Res.*, 99, 20,601–20,622, 1994.
- Gardner, C. S., C. A. Hostetler, and S. Lintelman, Influence of the mean wind field on the separability of atmospheric perturbation spectra, *J. Geophys. Res.*, 98, 8859–8872, 1993.
- Gossard, E. E., and W. H. Hooke, *Waves in the Atmosphere*, 456 pp., Elsevier, New York, 1975.
- Hamilton, K., Climatological statistics of stratospheric inertia-gravity waves deduced from historical rocketsonde wind and temperature data, *J. Geophys. Res.*, 96, 20,831–20,839, 1991.
- Hillert, W., F.-J. Lübken, and G. Lehmacher, TOTAL: A rocket-borne instrument for high resolution measurements of neutral air turbulence during DYANA, *J. Atmos. Terr. Phys.*, 56, 1835–1852, 1994.
- Hines, C. O., Tropopause mountain waves over Arecibo: A case study, *J. Atmos. Sci.*, 46, 476–488, 1989.
- Hines, C. O., The saturation of gravity waves in the middle atmosphere, I, Critique of linear-instability theory, *J. Atmos. Sci.*, 48, 1348–1359, 1991a.
- Hines, C. O., The saturation of gravity waves in the middle atmosphere, II, Development of Doppler-spread theory, *J. Atmos. Sci.*, 48, 1360–1379, 1991b.
- Hines, C. O., Pseudosaturation of gravity waves in the middle atmosphere: An interpretation of certain lidar observations, *J. Atmos. Terr. Phys.*, 55, 441–445, 1993a.
- Hines, C. O., The saturation of gravity waves in the middle atmosphere, IV, Cutoff of the incident wave spectrum, *J. Atmos. Sci.*, 50, 3045–3060, 1993b.
- Hirota, I., Climatology of gravity waves in the middle atmosphere, *J. Atmos. Terr. Phys.*, 46, 767–773, 1984.
- Holton, J. R., The influence of gravity wave breaking on the general circulation of the middle atmosphere, *J. Atmos. Sci.*, 40, 2497–2507, 1983.
- Holton, J. R., *An Introduction to Dynamic Meteorology*, 3rd ed., Academic, San Diego, Calif., 1992.
- Hooke, W. H., and K. R. Hardy, Further study of the atmospheric gravity waves over the eastern seaboard on 18 March 1969, *J. Appl. Meteorol.*, 14, 31–38, 1975.
- Hostetler, C. A., and C. S. Gardner, Observations of horizontal and vertical wave number spectra of gravity wave motions in the stratosphere and mesosphere over the mid-Pacific, *J. Geophys. Res.*, 99, 1283–1302, 1994.

- Huang, C. M., F. S. Kuo, H. Y. Lue, and C. H. Liu, Numerical simulations of the saturated gravity wave spectra in the atmosphere, *J. Atmos. Terr. Phys.*, *54*, 129–142, 1992.
- King, J. C., S. D. Mobbs, M. S. Darby, and J. M. Rees, Observations of an internal gravity wave in the lower troposphere at Halley, Antarctica, *Boundary Layer Meteorol.*, *39*, 1–13, 1987.
- Kitamura, Y., and I. Hirota, Small-scale disturbances in the lower stratosphere revealed by daily rawin sonde observations, *J. Meteorol. Soc. Jpn.*, *67*, 817–830, 1989.
- Kuo, F. S., and H. Y. Lue, Effect of wave-shear interaction on gravity wave activity in the lower and middle atmosphere, *J. Atmos. Terr. Phys.*, *56*, 1147–1155, 1994.
- Kuo, F. S., H. Y. Lue, C. M. Huang, C. L. Lo, C. H. Liu, S. Fukao, and Y. Muraoka, A study of velocity fluctuation spectra in the troposphere and lower stratosphere using MU radar, *J. Atmos. Terr. Phys.*, *54*, 31–48, 1992.
- Labitzke, K., Stratospheric-mesospheric midwinter disturbances: A summary of observed characteristics, *J. Geophys. Res.*, *86*, 9665–9678, 1981.
- Lefrère, J., and C. Sidi, Distortion of gravity wave spectra measured from ground-based stations, *Geophys. Res. Lett.*, *17*, 1581–1584, 1990.
- Lindzen, R. S., Turbulence and stress owing to gravity wave and tidal breakdown, *J. Geophys. Res.*, *86*, 9707–9714, 1981.
- Lindzen, R. S., Multiple gravity wave breaking levels, *J. Atmos. Sci.*, *42*, 301–305, 1985.
- Lu, W., and D. C. Fritts, Spectral estimates of gravity wave energy and momentum fluxes, III, Gravity wave-tidal interactions, *J. Atmos. Sci.*, *50*, 3714–3727, 1993.
- Lübken, F.-J., et al., Mean state densities, temperatures and winds during the MAC/SINE and MAC/EPSILON campaigns, *J. Atmos. Terr. Phys.*, *52*, 955–970, 1990.
- Marks, C. J., Some features of the climatology of the middle atmosphere revealed by Nimbus 5 and 6, *J. Atmos. Sci.*, *46*, 2485–2508, 1989.
- Marks, C. J., and M. J. Revell, A critical analysis of a month-long cyclonic anomaly in the New Zealand-Tasman Sea region using isentropic vorticity budgets, *Mon. Weather Rev.*, *122*, 2762–2776, 1994.
- Marsh, A. K. P., N. J. Mitchell, and L. Thomas, Lidar studies of stratospheric gravity-wave spectra, *Planet. Space Sci.*, *39*, 1541–1548, 1991.
- Maslowe, S. A., Critical layers in shear flows, *Ann. Rev. Fluid Mech.*, *18*, 405–432, 1986.
- Meyer, W., C. R. Philbrick, J. Röttger, R. Rüster, H.-U. Widdel, and F. J. Schmidlin, Mean winds in the winter middle atmosphere above northern Scandinavia, *J. Atmos. Terr. Phys.*, *49*, 675–687, 1987.
- Mitchell, N. J., L. Thomas, and A. K. P. Marsh, Lidar observations of long-period gravity waves in the stratosphere, *Ann. Geophys.*, *9*, 588–596, 1991.
- Mitchell, N. J., L. Thomas, and I. T. Prichard, Gravity waves in the stratosphere and troposphere observed by lidar and MST radar, *J. Atmos. Terr. Phys.*, *56*, 939–947, 1994.
- Müller, P., G. Holloway, F. S. Henyey, and N. Pomphrey, Nonlinear interactions among internal gravity waves, *Rev. Geophys.*, *24*, 493–536, 1986.
- Murayama, Y., T. Tsuda, and S. Fukao, Seasonal variation of gravity wave activity in the lower atmosphere observed with the MU radar, *J. Geophys. Res.*, *99*, 23,057–23,069, 1994.
- Nastrom, G. D., and D. C. Fritts, Sources of mesoscale variability of gravity waves, I, Topographic excitation, *J. Atmos. Sci.*, *49*, 101–110, 1992.
- Pfister, L., K. R. Chan, T. P. Bui, S. Bowen, M. Legg, B. Gary, K. Kelly, M. Proffitt, and W. Starr, Gravity waves generated by a tropical cyclone during the STEP tropical field program: A case study, *J. Geophys. Res.*, *98*, 8611–8638, 1993.
- Rind, D., R. Suozzo, N. K. Balachandran, A. Lacis, and G. Russell, The GISS global climate-middle atmosphere model, I, Model structure and climatology, *J. Atmos. Sci.*, *45*, 329–370, 1988.
- Röttger, J., and W. Meyer, Tidal wind observations with incoherent scatter radar and meteorological rockets during MAP/WINE, *J. Atmos. Terr. Phys.*, *49*, 689–703, 1987.
- Sato, K., A statistical study of the structure, saturation and sources of inertio-gravity waves in the lower stratosphere observed with the MU radar, *J. Atmos. Terr. Phys.*, *56*, 755–774, 1994.
- Sato, K., and M. Yamada, Vertical structure of atmospheric gravity waves revealed by the wavelet analysis, *J. Geophys. Res.*, *99*, 20,623–20,631, 1994.
- Schoeberl, M. R., The penetration of mountain waves into the middle atmosphere, *J. Atmos. Sci.*, *42*, 2856–2864, 1985a.
- Schoeberl, M. R., A ray tracing model of gravity wave propagation and breakdown in the middle atmosphere, *J. Geophys. Res.*, *90*, 7999–8010, 1985b.
- Senft, D. C., and C. S. Gardner, Seasonal variability of gravity wave activity and spectra in the mesopause region at Urbana, *J. Geophys. Res.*, *96*, 17,229–17,264, 1991.
- Senft, D. C., C. A. Hostetler, and C. S. Gardner, Characteristics of gravity wave activity and spectra in the upper stratosphere and upper mesosphere at Arecibo during early April 1989, *J. Atmos. Terr. Phys.*, *55*, 425–439, 1993.
- Senft, D. C., G. C. Papen, C. S. Gardner, J. R. Yu, D. A. Krueger, and C. Y. She, Seasonal variations of the thermal structure of the mesopause region at Urbana, IL (40°N, 88°W) and Ft. Collins, CO (41°N, 105°W), *Geophys. Res. Lett.*, *21*, 821–824, 1994.
- Shibata, T., S. Ichimori, T. Narikiyo, and M. Maeda, Spectral analysis of vertical temperature profiles observed by a lidar in the upper stratosphere and the lower mesosphere, *J. Meteorol. Soc. Jpn.*, *66*, 1001–1005, 1988.
- Smith, R. K., M. J. Reeder, N. J. Tapper, and D. R. Christie, Central Australian cold fronts, *Mon. Weather Rev.*, *123*, 16–38, 1995.
- Smith, S. A., D. C. Fritts, and T. E. VanZandt, Evidence of a saturated spectrum of atmospheric gravity waves, *J. Atmos. Sci.*, *44*, 1404–1410, 1987.
- Thayaparan, T., W. K. Hocking, and J. MacDougall, Observational evidence of tidal/gravity wave interactions using the UWO 2 MHz radar, *Geophys. Res. Lett.*, *22*, 373–376, 1995.
- Tsuda, T., T. Inoue, D. C. Fritts, T. E. VanZandt, S. Kato, T. Sato, and S. Fukao, MST radar observations of a saturated gravity wave spectrum, *J. Atmos. Sci.*, *46*, 2440–2447, 1989.
- Tsuda, T., T. E. VanZandt, M. Mizumoto, S. Kato, and S. Fukao, Spectral analysis of temperature and Brunt-Väisälä frequency fluctuations observed by radiosondes, *J. Geophys. Res.*, *96*, 17,265–17,278, 1991.
- Tsuda, T., Y. Murayama, K.-I. Oyama, F. J. Schmidlin, M. Bittner, H. Kanzawa, T. Nakamura, M. D. Yamanaka, S. Fukao, and S. Kato, Rocketsonde observations of the middle atmosphere dynamics at Uchinoura (31°N, 131°E) during the DYANA campaign, II, Characteristics of gravity waves, *J. Geomagn. Geoelectr.*, *44*, 1009–1023, 1992.
- Tsuda, T., Y. Murayama, H. Wiryosumarto, S. W. B. Harijono, and S. Kato, Radiosonde observations of equatorial atmosphere dynamics over Indonesia, 1, Equatorial waves and diurnal tides, *J. Geophys. Res.*, *99*, 10,491–10,505, 1994a.
- Tsuda, T., Y. Murayama, H. Wiryosumarto, S. W. B. Harijono, and S. Kato, Radiosonde observations of equatorial atmosphere dynamics over Indonesia, 2, Characteristics of gravity waves, *J. Geophys. Res.*, *99*, 10,507–10,516, 1994b.
- Uccellini, L. W., and S. E. Koch, The synoptic setting and possible energy sources for mesoscale wave disturbances, *Mon. Weather Rev.*, *115*, 721–729, 1987.
- VanZandt, T. E., A universal spectrum of buoyancy waves in the atmosphere, *Geophys. Res. Lett.*, *9*, 575–578, 1982.
- vonZahn, U., and W. Meyer, Mesopause temperatures in polar summer, *J. Geophys. Res.*, *94*, 14,647–14,651, 1989.
- Walterscheid, R. L., and G. Schubert, Nonlinear evolution of an upward propagating gravity wave: Overturning, convection, transience, and turbulence, *J. Atmos. Sci.*, *47*, 101–125, 1990.
- Weinstock, J., Saturated and unsaturated spectra of gravity waves, and scale dependent diffusion, *J. Atmos. Sci.*, *47*, 2211–2225, 1990.
- Whiteway, J. A., and A. I. Carswell, Rayleigh lidar observations of thermal structure and gravity wave activity in the high Arctic during a stratospheric warming, *J. Atmos. Sci.*, *51*, 3122–3136, 1994.
- Wilson, R., A. Hauchecorne, and M. L. Chanin, Gravity wave spectra in the middle atmosphere as observed by Rayleigh lidar, *Geophys. Res. Lett.*, *17*, 1585–1588, 1990.
- Wilson, R., M. L. Chanin, and A. Hauchecorne, Gravity waves in the middle atmosphere observed by Rayleigh lidar, 1, Case studies, *J. Geophys. Res.*, *96*, 5153–5167, 1991a.
- Wilson, R., M. L. Chanin, and A. Hauchecorne, Gravity waves in

- the middle atmosphere observed by Rayleigh lidar, 2, *Climatology, J. Geophys. Res.*, **96**, 5169–5183, 1991b.
- Wu, Y.-F., and H.-U. Widdel, Observational evidence of a saturated gravity wave spectrum in the mesosphere, *J. Atmos. Terr. Phys.*, **51**, 991–996, 1989.
- Wu, Y.-F., and H.-U. Widdel, Spectral analysis of atmospheric velocity fluctuations in the mesosphere, *J. Atmos. Terr. Phys.*, **52**, 23–33, 1990.
- Wu, Y.-F., and H.-U. Widdel, Further study of a saturated gravity wave spectrum in the mesosphere, *J. Geophys. Res.*, **96**, 9263–9272, 1991.
- Yamanaka, M. D., S. Fukao, H. Matsumoto, T. Sato, T. Tsuda, and S. Kato, Internal gravity wave selection in the upper troposphere and lower stratosphere observed by the MU radar, *Pure. Appl. Geophys.*, **130**, 481–495, 1989.
- Zhu, X., A new theory of the saturated gravity wave spectrum for the middle atmosphere, *J. Atmos. Sci.*, **51**, 3615–3626, 1994.
-
- S. D. Eckermann, Computational Physics, Inc., Suite 600, 2750 Prosperity Avenue, Fairfax, VA 22031, and E. O. Hulburt Center for Space Research, Code 7641, Naval Research Laboratory, Washington, DC 20375. (e-mail: eckerman@ismap4.nrl.navy.mil)

(Received November 2, 1994; revised March 8, 1995; accepted March 8, 1995.)